
SiMPO: Measure Matching for Online Diffusion Reinforcement Learning

Haitong Ma^{*1} Chenxiao Gao^{*2} Tianyi Chen² Na Li¹ Bo Dai²

Abstract

A commonly used family of RL algorithms for diffusion policies conducts softmax reweighting over the behavior policy, which usually induces an over-greedy policy and fails to leverage feedback from negative samples. In this work, we introduce *Signed Measure Policy Optimization (SiMPO)*, a simple and unified framework that generalizes reweighting scheme in diffusion RL with general monotonic functions. SiMPO revisits diffusion RL via a two-stage measure matching lens. First, we construct a virtual target policy by f -divergence regularized policy optimization, where we can relax the non-negativity constraint to allow for a signed target measure. Second, we use this signed measure to guide diffusion or flow models through reweighted matching. This formulation offers two key advantages: **a**) it generalizes to arbitrary monotonically increasing weighting functions; and **b**) it provides a principled justification and practical guidance for negative reweighting. Furthermore, we provide geometric interpretations to illustrate how negative reweighting actively repels the policy from suboptimal actions. Extensive empirical evaluations demonstrate that SiMPO achieves superior performance by leveraging these flexible weighting schemes, and we provide practical guidelines for selecting reweighting methods tailored to the reward landscape.

1. Introduction

Diffusion models (Ho et al., 2020; Song & Ermon, 2019) and flow models (Liu et al., 2022; Lipman et al., 2022) have emerged as a dominant class of generative models for synthesizing high-fidelity data across various modalities, from photorealistic imagery to complex structural biology. Beyond traditional density estimation, there is an increasing demand to align these models with specific downstream objectives—such as human preferences (Rafailov et al., 2023), biological evaluations (Avsec et al., 2021), and real-world physical feedback (Lei et al., 2025). Consequently, Rein-

forcement Learning (RL) for diffusion models has become a critical research direction for the downstream alignment.

The existing RL algorithms for diffusion models generally fall into two categories. One prominent direction treats the denoising reverse process as a Markov Decision Process (MDP) and optimizes the model using Policy Gradient algorithms (Black et al., 2023; Fan et al., 2023; Ren et al., 2024; Liu et al., 2025; Zhang et al., 2025b). These methods are often computationally intensive, requiring backpropagation through multiple sampling timesteps. Furthermore, they frequently mandate the use of Stochastic Differential Equation (SDE) samplers during training, which requires a very different training infrastructure. Moreover, the method relies on an underlying reverse Kullback-Leibler (KL) regularization with “mode-seeking” behavior, which encourages the model to stay close to its pre-trained initialization and limits the exploration.

An alternative and more efficient approach directly reweights the current behavior policies (Ma et al., 2025a; Tang et al., 2025), also known as Advantage Weighted Regression (AWR, Peng et al., 2019), which reweights the Evidence Lower Bound (ELBO) objective by advantage A (e.g., softmax reweighting by $\text{softmax}(A/\lambda)$). This framework, rooted in forward-KL regularization, is highly scalable and allows the RL algorithms to leverage the existing training infrastructure of diffusion models. However, this efficiency comes at a cost: the exponential weights usually assign high weights to a few good samples with high advantages but very small weights to all other samples, resulting in a greedy policy update (Mei et al., 2020) and ignoring negative samples (Frans et al., 2025).

To address the inherent limitations of softmax reweighting, we introduce *Signed Measure Policy Optimization (SiMPO)*, a unified framework that significantly broadens the scope of online diffusion RL. We propose a general two-stage framework: (a) a *construction* stage that derives a virtual *target measure* by solving an f -divergence regularized objective, where we relax the standard non-negativity constraint to allow for signed measures; and (b) a *projection* stage that projects this signed target back to the space of valid probability measures via reweighted flow matching. We show that SiMPO unifies existing reweighting (Ding et al., 2024; Ma et al., 2025a; Tang et al., 2025) while offering two distinct

^{*}Equal contribution ¹Harvard University. ²Georgia Institute of Technology.

advantages: **a)** It generalizes reweighting to *arbitrary monotonically increasing functions*, decoupling the method from rigid exponential scaling and allowing it to be tailored to specific problem landscapes; and **b)** It provides a *principled justification* for negative reweighting through the theory of signed measures. We further provide geometric interpretations illustrating how this mechanism actively ‘repels’ the policy from undesirable regions when training with negative reweighted flow matching. Finally, we provide comprehensive experimental results on bandit, MuJoCo locomotion tasks, and fine-tuning DNA sequence generation models to validate our approach. We demonstrate that SiMPO achieves superior performance by leveraging flexible and negative reweighting schemes, and we offer practical guidelines for selecting the optimal reweighting function based on the reward landscape.

Due to space limit, more related works is presented in Appendix A.

2. Preliminaries

2.1. Reinforcement Learning

Markov Decision Processes (MDPs). We consider Markov decision process (Puterman, 2014) specified by a tuple $\mathcal{M} = (\mathcal{S}, \mathcal{A}, r, P, \mu_0, \gamma)$, where \mathcal{S} is the state space, \mathcal{A} is the action space, $r : \mathcal{S} \times \mathcal{A} \rightarrow \mathbb{R}$ is a reward function, $P : \mathcal{S} \times \mathcal{A} \rightarrow \Delta(\mathcal{S})$ is the transition operator with $\Delta(\mathcal{S})$ as the family of distributions over \mathcal{S} , $\mu_0 \in \Delta(\mathcal{S})$ is the initial distribution and $\gamma \in (0, 1)$ is the discount factor.

KL-regularized policy optimization (Tomar et al., 2021; Lan, 2023; Peters et al., 2010) is closely related to practical proximity-based algorithms such as TRPO (Schulman, 2015) and PPO (Schulman et al., 2017), but with a different approach to enforce the proximity constraints. The policy update is formulated as

$$\pi = \operatorname{argmax}_{\pi: \mathcal{S} \rightarrow \Delta(\mathcal{A})} \mathbb{E}_{\mathbf{a} \sim \pi} [Q^{\pi_{\text{old}}}(\mathbf{s}, \mathbf{a})] - \lambda D_{\text{KL}}(\pi \| \pi_{\text{old}}; \mathbf{s}) \quad (1)$$

where $Q^{\pi_{\text{old}}}(\mathbf{s}, \mathbf{a}) = \mathbb{E}_{\pi_{\text{old}}}[\sum_{\tau=0}^{\infty} \gamma^{\tau} r(\mathbf{s}_{\tau}, \mathbf{a}_{\tau}) | \mathbf{s}_0 = \mathbf{s}, \mathbf{a}_0 = \mathbf{a}]$ is the state-action value function and π_{old} is the current policy, $\lambda \in \mathbb{R}^+$ is the regularization strength. The additional KL divergence objective constrains the updated policy to be approximately within the trust region.

The closed-form solution of policy mirror descent (1) is a **softmax reweighted** version of the current policy:

$$\pi^*(\mathbf{a} | \mathbf{s}) = \pi_{\text{old}}(\mathbf{a} | \mathbf{s}) \frac{\exp(Q^{\pi_{\text{old}}}(\mathbf{s}, \mathbf{a}) / \lambda)}{Z(\mathbf{s})}, \quad (2)$$

and $Z(\mathbf{s}) = \int \pi_{\text{old}}(\mathbf{a} | \mathbf{s}) \exp(Q^{\pi_{\text{old}}}(\mathbf{s}, \mathbf{a}) / \lambda) d\mathbf{a}$ is the partition function. It is often referred to as weighted behavior cloning or advantage-weighted regression in recent literature (Peng et al., 2019; Frans et al., 2025; Wang et al., 2018; Physical Intelligence et al., 2025; Siegel et al., 2020; Nair

et al., 2020).

2.2. Diffusion and Flow Models

Diffusion models (Ho et al., 2020; Song & Ermon, 2019) or flow models (Lipman et al., 2022; Liu et al., 2022) learn continuous data distributions by gradually perturbing clean data $\mathbf{x}_0 \sim p_{\text{data}}$ with Gaussian noise according to a forward process:

$$\mathbf{x}_t = \alpha_t \mathbf{x}_0 + \sigma_t \boldsymbol{\epsilon}, \boldsymbol{\epsilon} \sim \mathcal{N}(\mathbf{0}, \mathbf{I}),$$

and then learn to reverse this process to sample from the target distribution p_{data} . In this paper, we employ the \mathbf{v} -prediction formulation, where the velocity \mathbf{v} is defined as the time-derivative of \mathbf{x} , *i.e.*, $\mathbf{v} = \dot{\alpha}_t \mathbf{x}_0 + \dot{\sigma}_t \boldsymbol{\epsilon}$. Diffusion models or flow models fit a parameterized network $D_{\theta}(\mathbf{x}_t, t)$ to match the marginal velocity field $\mathbf{v}_t(\mathbf{x}_t)$:

$$\mathbf{v}_t(\mathbf{x}_t) = \mathbb{E}_{\mathbf{x}_0 \sim p_{0|t}} [\mathbf{v}_{t|0}(\mathbf{x}_t | \mathbf{x}_0)], \quad (3)$$

where $p_{0|t}$ is the posterior distribution given \mathbf{x}_t , $\mathbf{v}_{t|0}(\mathbf{x}_t | \mathbf{x}_0)$ is the conditional velocity field

$$\mathbf{v}_{t|0}(\mathbf{x}_t | \mathbf{x}_0) = \frac{(\sigma_t \dot{\alpha}_t - \dot{\sigma}_t \alpha_t)}{\sigma_t} \mathbf{x}_0 + \frac{\dot{\sigma}_t}{\sigma_t} \mathbf{x}_t.$$

However, the marginal velocity field is not tractable due to the posterior distribution, therefore in practice, we employ the conditional velocity field matching, which is equivalent up to some constant:

$$\mathcal{L}(\theta) = \mathbb{E}_{\mathbf{x}_0, \boldsymbol{\epsilon}} [\|D_{\theta}(\mathbf{x}_t, t) - \mathbf{v}_{t|0}\|^2].$$

After training is complete, sampling is done by solving a stochastic or ordinary differential equation (SDE/ODE), for example $d\mathbf{x}_t/dt = D_{\theta}(\mathbf{x}_t, t)$.

Different specifications of the noise schedule $\{(\alpha_t, \sigma_t)\}$ leads to different methods. For example, the variance-exploding (VE) diffusion model (Song & Ermon, 2019) has the schedule $\alpha_t = 1$ and $\sigma_t = \sqrt{t}$. Flow models (Lipman et al., 2022; Liu et al., 2022) employ linear interpolation with $\alpha_t = 1 - t$, $\sigma_t = t$, which simplifies the conditional velocity target to $\mathbf{v}_{t|0} = \boldsymbol{\epsilon} - \mathbf{x}_0$. Note that diffusion models may also employ \mathbf{x}_0 - or $\boldsymbol{\epsilon}$ -prediction, which are equivalent to \mathbf{v} -prediction used in this paper due to the reparameterization among the three (Li & He, 2025).

2.3. f -divergence and Extension to Signed Measure

Divergence describes the difference between two probability distributions. A general family of divergences is the f -divergences (Csiszár & Shields, 2004; Liese & Vajda, 2006), also known as the Ali-Silvey distances (Ali & Silvey, 1966). For a convex function $f : \mathbb{R}^+ \rightarrow \mathbb{R}$ with $f(1) = 0$, the corresponding f -divergence for two distributions p, q is defined as:

$$D_f(p \| q) = \mathbb{E}_{q(x)} \left[f \left(\frac{p(x)}{q(x)} \right) \right],$$

where f is called the generator function. Notice that the generator function is not unique; by definition, $\tilde{f}(x) = f(x) + C(x - 1)$ yields the same divergence as $f(x)$ when

C is a constant. Different choices of f -divergence can cover a wide class of popular divergences, which we summarize in Table 1.

Table 1. A few examples of f -divergence, their generator functions and the resulting reweighting factor.

Divergence D_f	Generator $f(x)$	Weighting Scheme $w(A)$
Forward KL Divergence	$x \log x$	$\exp(\hat{A})$
χ^2 -Divergence	$x^2 - 1$	$\text{ReLU}(\hat{A})$
α -Divergence ($\alpha > 1$)	$\frac{x^\alpha - x}{\alpha(\alpha-1)}$	$\text{ReLU}(\hat{A})^{1/(\alpha-1)}$ *

Extension to p being a signed measure (Csiszár et al., 2002; Broniatowski & Keziou, 2006). The definition of f -divergence usually consider p, q both as probability measures, which are non-negative. Extending the definition of f -divergences to cases where p is a finite signed measure while q is still a probability measure also holds under mild conditions, such as f being a measurable function on \mathbb{R}^1 . Following Broniatowski & Keziou (2006), we call this the f -divergence on signed measures, to distinguish it from the standard definition.

3. A Unified Framework for Reweighting with Measure Matching

In this section, we generalize reweighting in diffusion RL beyond enforcing a valid probability distribution such as Equation (2). We show that we can first construct a *signed, un-normalized target measure*, and then project the measure back onto the probability simplex via *reweighted flow matching* (see Figure 1). This framework unifies existing diffusion policy optimization methods and inspire novel reweighting schemes, such as new reweighting functions and negative reweighting. We also provide geometric interpretation of negative reweighted flow matching.

3.1. A Two-Stage Framework for Diffusion Policy Optimization

Consider the policy optimization problem with f -divergence regularization

$$\max_{\pi \in \Pi} \mathbb{E}_{\pi} [Q(\mathbf{s}, \mathbf{a})] - \lambda D_f(\pi \| \pi_{\text{old}}). \quad (4)$$

Here, we assume $f : \mathbb{R}^+ \rightarrow \mathbb{R}$ is strictly convex and differentiable and $f(1) = 0$. The policy $\pi : \mathcal{S} \rightarrow \Delta(\mathcal{A})$ maps each state \mathbf{s} to a probability distribution over the action space, and thus satisfies the normalization constraint $\int \pi(\mathbf{a}|\mathbf{s}), d\mathbf{a} = 1$ and the non-negativity constraint $\pi(\mathbf{a}|\mathbf{s}) \geq 0$ for all $\mathbf{s} \in \mathcal{S}$.

To solve this problem for diffusion-based policies, we adopt a two-stage decomposition.

Stage I: Defining the optimal target policy π^* via reweighting. By converting the constrained optimization

problem in (4) into an unconstrained one via a Lagrangian formulation, we can show that the optimal target policy admits the form

$$\pi^*(\mathbf{a}|\mathbf{s}) = \pi_{\text{old}}(\mathbf{a}|\mathbf{s}) \bar{g}_f \left(\frac{Q(\mathbf{s}, \mathbf{a}) - \nu(\mathbf{s})}{\lambda} \right), \quad (5)$$

where $\nu : \mathcal{S} \rightarrow \mathbb{R}$ are multipliers whose actual values depend on λ and Q , and \bar{g}_f is the *clipped inverse derivative* function satisfying

$$\bar{g}_f(x) = \begin{cases} (f')^{-1}(x) & \text{if } x > f'(0) \\ 0 & \text{if } x \leq f'(0) \end{cases}. \quad (6)$$

The detailed derivation is deferred to Appendix C.1.

Stage II: Projection via reweighted flow matching. Although (5) provides an analytic expression for the target policy π^* , we still need to project it back to the hypothesis space defined by our parameterization. To achieve this, we employ the simple and commonly used reweighted flow matching (Ding et al., 2024; Ma et al., 2025a):

$$\mathcal{L}(\theta) = \mathbb{E}_{\mathbf{s}, \mathbf{a}_0, \epsilon} [w(\mathbf{s}, \mathbf{a}) \| D_{\theta}(\mathbf{s}, \mathbf{a}_t, t) - \mathbf{v}_{t|0} \|^2] \quad (7)$$

where $w(\mathbf{s}, \mathbf{a}) = \bar{g}_f \left(\frac{Q(\mathbf{s}, \mathbf{a}) - \nu(\mathbf{s})}{\lambda} \right)$ is the reweighting factor in (5). In Appendix D, we show that the closed-form solution of the reweighted conditional flow matching objective is given by a weighted average of conditional velocities under the posterior distribution $p_{0|t}$ induced by the old policy π_{old} :

$$D_{\theta}^*(\mathbf{s}, \mathbf{a}_t, t) = \frac{\mathbb{E}_{\mathbf{a}_0 \sim p_{0|t}} [w(\mathbf{s}, \mathbf{a}_0) \mathbf{v}_{t|0}(\mathbf{a}_t | \mathbf{a}_0)]}{\mathbb{E}_{\mathbf{a}_0 \sim p_{0|t}} [w(\mathbf{s}, \mathbf{a}_0)]}. \quad (8)$$

Compared to the unweighted formulation (3), this solution reweights the conditional velocity according to its value, thereby emphasizing actions with higher advantage.

Most importantly, such two-stage perspective elucidates the design space underlying a broad class of existing algorithms. In what follows, we show that several previously proposed methods can be recovered as special cases of our framework. Moreover, this formulation naturally extends to signed measures, offering a principled way to incorporate negative samples into training.

3.2. Unifying Existing Reweighting Schemes via f -Divergences

By choosing the f -divergence to be the forward KL divergence, we recover the KL-regularized objective used in AWR (Peng et al., 2019) and DPMD (Ma et al., 2025a).

Example 3.1 (DPMD (Ma et al., 2025a) as forward KL-regularization). Let $D_f = D_{\text{KL}}$, therefore $f(x) = x \log x - x + 1$, $g_f(x) = \exp(x)$, and $f'(0) = -\infty$. Recognizing $\nu(\mathbf{s})$ as the normalization factor $Z(\mathbf{s})$, we can recover DPMD by

$$\mathcal{L}_{\text{DPMD}}(\theta) = \mathbb{E}_{\mathbf{s}, \mathbf{a}_0, \epsilon} \left[\frac{\exp(Q(\mathbf{s}, \mathbf{a}))}{Z(\mathbf{s})} \| D_{\theta}(\mathbf{s}, \mathbf{a}_t, t) - \mathbf{v}_{t|0} \|^2 \right].$$

¹Details can be found in Appendix B.

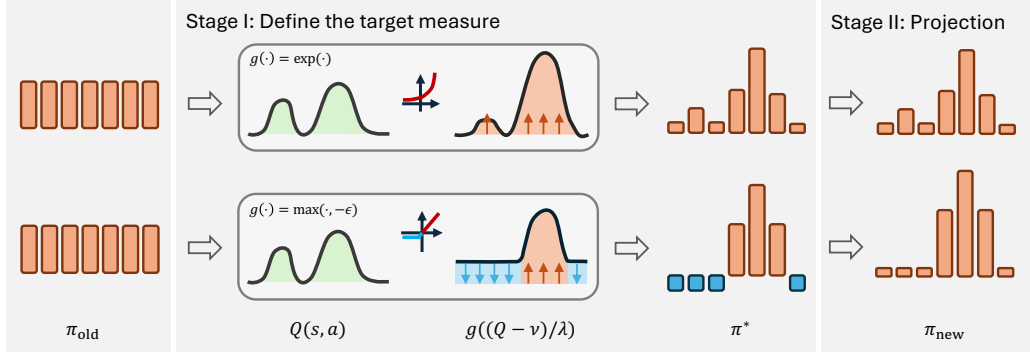


Figure 1. A demonstrative comparison between the existing advantage-weighted regression (**up**) and the proposed SiMPO framework (**down**). We employ a two-stage viewpoint, via first creating a target measure that can be signed or unnormalized and projecting it back to probability distributions by reweighted conditional flow matching. Especially, the negative weights have a “repelling” effect, pushing the generated action away from negative samples, enhancing algorithm performance.

Moreover, we can see QVPO (Ding et al., 2024), originally derived from a lower bound of policy gradient objective, as a special case with χ^2 divergence.

Example 3.2 (QVPO (Ding et al., 2024) as χ^2 regularization.). Let D_f be the χ^2 -divergence by setting $f(x) = x^2 - 1$, $g_f(x) = \frac{1}{2}x$, and $f'(0) = 0$. The QVPO objective

$$\mathcal{L}_{\text{QVPO}}(\theta) =$$

$$\mathbb{E}_{\mathbf{s}, \mathbf{a}_0, \epsilon} \left[[Q(\mathbf{s}, \mathbf{a}) - V(\mathbf{s})]_+ \|D_\theta(\mathbf{s}, \mathbf{a}_t, t) - \mathbf{v}_{t|0}\|^2 \right]$$

can be recovered by fixing $\lambda = \frac{1}{2}$, where $[\cdot]_+ = \max(\cdot, 0)$.

Noticing that both the KL-divergence and χ^2 -divergence are special cases of α -divergence, we can employ a more general regularization family and weighting scheme.

Example 3.3 (Power function reweighting as α -divergence regularization). For general α -divergences with $\alpha > 1$, we have $f(x) = \frac{x^{\alpha-1}}{(\alpha-1)\alpha}$, which induces $f'(0) = 0$ and $g_f(x) = (\alpha - 1)x^{\frac{1}{\alpha-1}}$. Therefore, we can get optimal policies reweighted by arbitrary power functions,

$$\pi(\mathbf{a}|\mathbf{s}) \propto \pi_{\text{old}}(\mathbf{a}|\mathbf{s}) \left[\frac{Q(\mathbf{s}, \mathbf{a}) - \nu(\mathbf{s})}{\lambda} \right]_+^{\frac{1}{\alpha-1}},$$

where certain constant factors are absorbed into λ . This suggests the following objective:

$$\mathcal{L}_\alpha(\theta) =$$

$$\mathbb{E}_{\mathbf{s}, \mathbf{a}_0, \epsilon} \left[\left[\frac{Q(\mathbf{s}, \mathbf{a}) - \nu(\mathbf{s})}{\lambda} \right]_+^{\frac{1}{\alpha-1}} \|D_\theta(\mathbf{s}, \mathbf{a}_t, t) - \mathbf{v}_{t|0}\|^2 \right].$$

By tuning α , we can shape the curvature of the weighting function to better match the characteristics of the underlying value landscape. With an appropriate choice of α , our approach can avoid both the overly flat weighting used in QVPO (Example 3.2) and the statistical instabilities induced by the exponential weighting in DPMD (Example 3.1).

3.3. Negative Reweighting by Extending f -divergence Definition to Signed Measures

One common drawback of the above methods is that their weighting functions effectively *rule out* the negative samples (as measured by the advantage function), due to the extremely small or zero weights assigned to them. Therefore, these methods cannot exploit the negative samples during training, and may therefore be more prone to getting trapped in local optima.

This issue stems from the non-negativity constraint of the target optimal policy $\pi^*(\mathbf{a}|\mathbf{s}) \geq 0$, which in turn forces the weight $g_f(\cdot)$ or $w(\cdot, \cdot)$ to be non-negative. However, since our framework decouples the algorithm into two stages, and the diffusion/flow policy implicitly performs sampling from a distribution, we can actually specify a target measure without the non-negativity constraint during **Stage I**, and then recover a valid probability distribution by fitting diffusion/flow policy via reweighted matching in **Stage II**, as shown in our illustrative comparison in Figure 1. This inspires us to shift our attention to optimization over normalized **signed measures** $\bar{\Pi} = \{\pi : \int \pi(\mathbf{a}|\mathbf{s}) = 1, \forall \mathbf{s} \in \mathcal{S}\}$. Moreover, because the key design choice is the weighting function $g_f = (f')^{-1}$, it is more principled to approach the problem directly through designing the weighting function.

Therefore, we consider relaxing the target measure to signed measures:

$$\pi^*(\mathbf{a}|\mathbf{s}) \propto \pi_{\text{old}}(\mathbf{a}|\mathbf{s}) g \left(\frac{Q(\mathbf{s}, \mathbf{a}) - \nu(\mathbf{s})}{\lambda} \right), \quad (9)$$

where the only requirement for $g(\cdot)$ is that it is monotonic increasing. Defining the weighting function $w(\mathbf{s}, \mathbf{a}) = g \left(\frac{Q(\mathbf{s}, \mathbf{a}) - \nu(\mathbf{s})}{\lambda} \right)$, we continue to optimize the policy via reweighted flow matching, as in (7). This substantially broadens the scope of our framework in two respects.

First, it allows us to adopt any monotonic increasing function as the weighting rule. *Second*, it enables the inclusion

of negative samples by permitting negative weights during training. We show that existing negative-aware reweighting scheme exactly fits into our framework,

Example 3.4 (*wdl* (Tang et al., 2025) as an example of negative reweighting). *wdl* (Tang et al., 2025) also incorporates negative reweighting to enhance the reasoning capability of diffusion language models. Their weighting function is defined as

$g(\hat{A}(\mathbf{s}, \mathbf{a}_i)) = \text{softmax}(\hat{A}(\mathbf{s}, \mathbf{a}_i)) - \text{softmax}(-\hat{A}(\mathbf{s}, \mathbf{a}_i))$
 where $\text{softmax}(\mathbf{s}, \mathbf{a}_i) = \frac{\exp(\hat{A}(\mathbf{s}, \mathbf{a}_i))}{\sum_i \exp(\hat{A}(\mathbf{s}, \mathbf{a}_i))}$ and $\hat{A}(\mathbf{s}, \mathbf{a}_i) = \frac{R(\mathbf{s}, \mathbf{a}_i) - \text{mean}(R(\mathbf{s}, \mathbf{a}_{1:G}))}{\text{std}(R(\mathbf{s}, \mathbf{a}_{1:G}))}$ is the group-relative advantage across a total number of G responses to the same query \mathbf{s} . Note that, $g(x)$ here is exactly monotonic increasing.

Finally, we show that, even without non-negativity constraints enforced, the target policy still improves over the current policy π_{old} as long as it is normalized $\int \pi(\mathbf{a}|\mathbf{s})d\mathbf{a} = 1$.

Theorem 3.5 (Guaranteed policy improvement, proof in Appendix C.3). *Assume g is strictly increasing, we have guaranteed policy improvement on π over π_{old} , i.e., $\mathbb{E}_\pi[Q(\mathbf{s}, \mathbf{a})] \geq \mathbb{E}_{\pi_{\text{old}}}[Q(\mathbf{s}, \mathbf{a})]$ for $\forall \mathbf{s} \in \mathcal{S}$.*

3.4. Geometric Interpretation of Negative Reweighted Flow Matching

Allowing $w(\mathbf{s}, \mathbf{a})$ be negative will also affect the optimal solution of conditional flow matching in Equation (8). We provide an geometric interpretation in this section. Compared to original optimal solution with non-negative weights in Equation (8), there are two cases if we consider weights being possibly negative, depending on the sign of denominator $\mathbb{E}_{\mathbf{a}_0 \sim p_{0|t}}[w(\mathbf{s}, \mathbf{a}_0)]$:

Case I: For all \mathbf{a}_t with $\mathbb{E}_{\mathbf{a}_0 \sim p_{0|t}}[w(\mathbf{s}, \mathbf{a}_0)] > 0$, the optimal weighted average solution in Equation (8) still holds. However, the negative weights will change the sign of $\mathbf{v}_{t|0}$ in the weighted average, pushing the weighted average velocity away from those $\mathbf{v}_{t|0}$ with negative weights.

Remark 3.6 (Another interpretation from generation of reweighted distributions via signed measures). Even when the weights $w(\mathbf{s}, \mathbf{a}_0)$ take negative values (as in **Case I**), the closed-form velocity field solution from Equation (8) generates a valid probability path ρ_t , provided the total measure remains positive. The generated path is given by:

$$\rho_t(\mathbf{a}|\mathbf{s}) = \frac{1}{Z(\mathbf{s})} \int w(\mathbf{s}, \mathbf{a}_0) \pi_{\text{old}}(\mathbf{a}_0|\mathbf{s}) p_{t|0}(\mathbf{a}|\mathbf{a}_0) d\mathbf{a}_0, \quad (10)$$

where $Z(\mathbf{s}) = \int w(\mathbf{s}, \mathbf{a}_0) \pi_{\text{old}}(\mathbf{a}_0|\mathbf{s}) d\mathbf{a}_0$ is the normalization constant. Mathematically, the negative weights introduce negative components to the integral. To satisfy the normalization constraint $\int \rho_t(\mathbf{a}|\mathbf{s}) d\mathbf{a} = 1$, the contribution from regions with positive weights must be amplified to offset the negative mass. Consequently, this mechanism ef-

fectively concentrates significantly higher probability mass on positive samples than standard reweighting.

Case II: For all \mathbf{a}_t with $\mathbb{E}_{\mathbf{a}_0 \sim p_{0|t}}[w(\mathbf{s}, \mathbf{a}_0)] \leq 0$, the loss is unbounded and have a ‘‘repelling’’ effect, consistently pushing D_θ away from the solution in (8), which means pushing generated path \mathbf{a}_t away from the negative weights region. The derivations are deferred to Appendix D.

In summary, in both cases the negative weights will *push the generated probability paths away from actions with negative weights*.

Repelling effect helps policy improvement. There are two possible outcomes from the repelling effect: **a)** pushing the actions towards higher advantages; **b)** pushing actions to regions not included in the support of old policy π_{old} , encouraging exploration. Both cases provide useful feedback from negative samples.

Algorithm 1 Signed Measure Policy Optimization (SiMPO)

Require: Q -function, current policy π_{old} , regularization strength λ , number of samples N

- 1: # Stage I: Create target measure
 - 2: sample N actions $\mathbf{a}_i \sim \pi(\cdot|\mathbf{s}), i = 1, \dots, N$ for each \mathbf{s}
 - 3: Evaluate $Q_i \doteq Q(\mathbf{s}, \mathbf{a}_i), i = 1, 2, \dots, N$
 - 4: Compute normalization factor $\nu(\mathbf{s})$
 - 5: Compute reweighting weights $w(\mathbf{s}, \mathbf{a}_i)$
 - 6: # Stage II: Reweighted Flow Matching
 - 7: Train policies by reweighted flow matching (7).
-

4. SiMPO: A Practical Algorithm

The pseudo-code of the SiMPO framework is presented in Algorithm 1. By instantiating the two-stage framework described in Section 3.1 with different weighting functions, we study several variants of SiMPO in this paper. Specifically, we consider: 1) **SiMPO-Exp**, which uses exponential weighting as DPMD; 2) **SiMPO-Linear** and **SiMPO-Square**, which uses power functions $w(\mathbf{s}, \mathbf{a}) = \left[\frac{Q(\mathbf{s}, \mathbf{a}) - \nu(\mathbf{s})}{\lambda} \right]_+$ and $w(\mathbf{s}, \mathbf{a}) = \left[\frac{Q(\mathbf{s}, \mathbf{a}) - \nu(\mathbf{s})}{\lambda} \right]_+^2$, respectively. For variants that allow negative weighting, as discussed in Section 3.4, negative weights must be carefully controlled to avoid destabilizing learning. To this end, we apply a simple truncation:

$$w(\mathbf{s}, \mathbf{a}) = \max\left(\frac{Q(\mathbf{s}, \mathbf{a}) - \nu(\mathbf{s})}{\lambda}, \ell\right), \quad (11)$$

where $\ell < 0$ determines the magnitude of negative weighting. We refer to this variant as **SiMPO-Lin. Neg.**

Normalization constraints It is not clear how to compute the normalization term $\nu(\mathbf{s})$ for general reweighting functions. We propose a population-based solution by estimating

the normalizer with a group of samples. For exponential weighting $g(\cdot) = \exp(\cdot)$, this translates to computing the softmax as the final weight; while for power function weighting, we can compute the normalizers by first determining the number of active samples (*i.e.*, samples that are not clipped), and then compute the exact value such that the weights are normalized. Details about this process, and also its generalization to accommodate negative values, can be found in Appendix E.

5. Experiments

In the experiments, we mainly answer the following questions:

- Q1** How do other regularization terms affect the overall performance?
- Q2** Does the negative weights help improve performance?
- Q3** How do we adapt reweighting functions according to the reward landscape?

5.1. Exploration-Exploitation Trade-off in Bandit

We first study **Q2** and **Q3** using a toy example, a one-dimensional bandit problem, with a given reward function $R(\cdot)$. The objective is defined as $\max_{\pi} \mathbb{E}_{a \sim \pi} [R(a)] - \lambda D_f(\pi \| \pi_{\text{old}})$. We evaluate performance using the simple expected regret metric, given by $\max_{a \in \mathcal{A}} R(a) - \mathbb{E}_{a \sim \pi} [R(a)]$.

The effect of negative weights on exploration. First, to answer **Q2**, we select a reward function with two optima, shown in Figure 2 (Left), and initialize the policy to be aligned with the sub-optimum, so the policy is very likely to get stuck at the sub-optimum. We compare four types of reweighting methods: **Linear Square**, **Exp** $w(a) = \text{softmax}(\hat{R}(a))$, and linear with negative $\ell = -0.05$ labeled as **Lin. Neg.** The regret curves are shown in Figure 2 (right), which show that, all reweighting methods cannot achieve the global optimum for every trial without negative reweighting; in particular, linear reweighting frequently becomes trapped in a local optimum. After adding negative reweighting, as shown in Figure 2 (right), **Lin. Neg.** can escape the sub-optimum, showing that negative reweighting can effectively help exploration.

Reweighting and reward landscape. Moreover, to answer **Q3**, we introduce another reward function, both illustrated in the left column of Figure 3: one characterized by two broad optima (top row) and the other by two sharp optima (bottom row). The policies are initialized as Gaussian distributions in the middle of two optima, so exploration is not necessary. We show three non-negative reweighting functions: **Linear**, **Square**, and **Exp**. The resulting expected simple regret curves are presented in the right column of Figure 3. For the broad optimum (top row), **Square** reweighting (induced by α -divergence with $\alpha = 1.5$) achieves the lowest

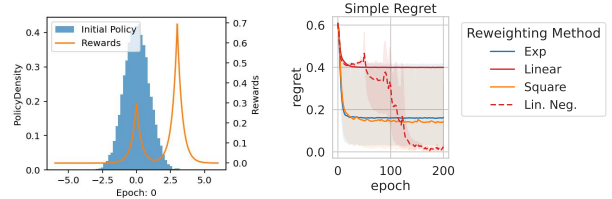


Figure 2. Bandit problem to answer **Q2**. **Left**: Reward functions and initial policy. **Right**: Regret curves comparing different reweighting with and without negative reweighting functions over 200 epochs.

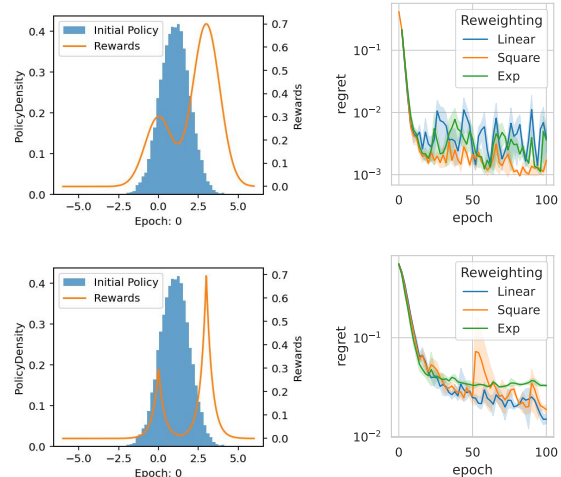


Figure 3. Demonstration of the first bandit problem exploring **Q2**. **Left column**: Reward functions (blue) showing broad (top) vs. sharp (bottom) optima, with initial policy distributions (histograms). **Right column**: Regret curves comparing different reweighting schemes over 100 epochs.

regret and more stable convergence. However, in the sharp optimum setting (bottom row), **Linear** reweighting demonstrates superior performance, maintaining consistently lower and more stable regret. In both cases, **Exp** reweighting is not optimal.

Therefore, we observe that the choice of regularization term is critical to the algorithm’s performance in online RL, as it governs the exploration-exploitation trade-off relative to the curvature of the reward function.

5.2. Locomotion Tasks

To answer all questions on standard RL benchmarks, we implemented our algorithm with the JAX package and evaluated the performance on 6 OpenAI Gym MuJoCo v4 tasks. All environments are trained with a total of 1 million environment interactions.

Baselines. The baselines include two families of model-free RL algorithms. The first family is diffusion policy RL, which includes a collection of recent diffusion-policy online RLs, including QSM (Psenka et al., 2023), QVPO (Ding

Table 2. Performance of 1M steps on Gym-MuJoCo environments. We report the average returns of the last checkpoint \pm standard deviation over 5 random seeds. **Orange** denotes our algorithms with different reweighting, while **blue** highlights our linear weighting with negative weights. **Bold** numbers indicates best mean returns and underlined numbers indicates mean returns within standard deviation of the best runs. All variants of the proposed **SiMPO** achieve consistently good performance on most tasks. Adding negative weights further improve performance on two tasks while not hurting performance on other tasks much.

Method	HALFCHEETAH	HUMANOID	ANT	WALKER2D	HOPPER	SWIMMER
Classic Model-Free RL						
TD3	9820 \pm 1543	<u>5263</u> \pm 47	4400 \pm 1196	3732 \pm 388	3387 \pm 302	88 \pm 25
SAC	10257 \pm 1057	<u>5298</u> \pm 69	2858 \pm 2637	4625 \pm 557	2126 \pm 1205	85 \pm 29
Diffusion RL Baselines						
QSM	12573 \pm 1197	2308 \pm 468	711 \pm 42	3933 \pm 185	1594 \pm 256	108 \pm 37
DIPO	10136 \pm 2525	<u>5184</u> \pm 132	977 \pm 20	3809 \pm 1112	1191 \pm 770	46 \pm 3
DACER	<u>13298</u> \pm 790	3142 \pm 2557	4887 \pm 646	1871 \pm 3131	1813 \pm 1781	116 \pm 12
QVPO	8081 \pm 701	1375 \pm 886	2122 \pm 2011	2866 \pm 490	960 \pm 414	83 \pm 36
Ours						
SiMPO-Exp	<u>13627</u> \pm 704	5100 \pm 238	5071 \pm 533	4616 \pm 145	3002 \pm 296	69 \pm 16
SiMPO-Square	<u>13276</u> \pm 1095	5068 \pm 435	5925 \pm 345	4478 \pm 1520	2809 \pm 954	52 \pm 1
SiMPO-Linear	<u>13636</u> \pm 521	<u>5376</u> \pm 154	5984 \pm 179	4909 \pm 186	2637 \pm 370	68 \pm 14
SiMPO-Lin. Neg.	13907 \pm 1902	5466 \pm 377	5700 \pm 230	<u>4906</u> \pm 438	2609 \pm 733	66 \pm 13

et al., 2024), DACER (Wang et al., 2024b), DIPO (Yang et al., 2023) and DPPO (Ren et al., 2024). The second family is classic model-free online RL baselines including PPO (Schulman et al., 2017), TD3 (Fujimoto et al., 2018) and SAC (Haarnoja et al., 2018). A more detailed explanation to the baselines can be found in Appendix F.1.

Q1 The results are summarized in Table 2. All three reweighting methods, **Linear**, **Square**, and **Exp**, exhibit consistently strong performance and outperform other diffusion-based RL baselines across most environments, with the exception of Swimmer. **Q2** Allowing negative weighting further enhances performance with $\ell = -0.05$ (**SiMPO-Lin. Neg.** in the table) achieves additional gains on HalfCheetah and Humanoid, while having minimal impact on the remaining tasks.

Q3 To see the effect of reward functions under different landscapes in locomotion tasks, we handcrafted different reward functions to change the landscape in two DeepMind Control Suite tasks (Tassa et al., 2018), Cheetah-Run and Walker-Run, shown in Figure 4. The task is to run as fast as possible, where rewards are monotonically increasing functions of robot speed. Four different rewards are ordered from flat to greedy as *sqrt*, *linear*, *square*, *exp*. The detailed definition of these reward functions are deferred to Appendix F.2.

The results are shown Figure 5, which shows that **Square** reweighting excels at flat reward functions such as *sqrt* and *linear*, while **Linear** reweighting has better performance on steep re-

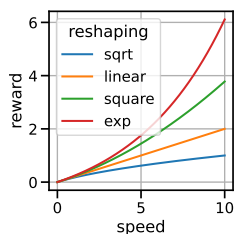


Figure 4. Reward functions.

ward functions, such as *exp*. The finding is consistent with our observations in the bandit problem. Therefore, we can choose **Linear** reweighting for steep reward landscapes and **Square** reweighting for relatively flat reward landscapes. Note that this is only qualitative intuitions rather than saying one reweighting function must be better than another.

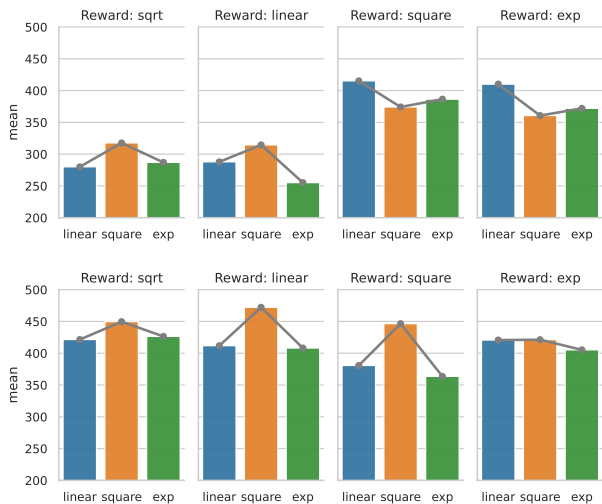


Figure 5. Performance with different reweighting functions with different reward functions on the Cheetah Run task. Square reweighting achieves the best performance with flat rewards, while linear reweighting achieves the best performance with steep rewards, both outperforming exponential reweighting.

5.3. DNA Sequence Generation

Finally, we evaluate our method on a real-world problem, learning to generate DNA sequences with a discrete diffusion model². The task is to fine-tune a DNA generation model, learned from a large public enhancer dataset containing roughly 700,000 DNA sequences (Gosai et al., 2023), to optimize the gene expression activity (Avsec et al., 2021). We leverage pretrained generation and reward models from (Wang et al., 2024a). We tested multiple variants of our algorithm, including **Linear**, **Square**, and their negative reweighting variants.

Baselines. We compare against controlled generation approaches including conditional guidance (CG, Nisonoff et al., 2024), SMC and TDS (Wu et al., 2023), and classifier-free guidance (CFG, Ho & Salimans, 2022), as well as a strong RL-based baseline, DRAKES (Wang et al., 2024a), which leveraged reparameterized policy gradient using Gumbel-softmax, and RL-D² (Ma et al., 2025b), which use weighted regression with KL divergence regularization (the same as **SiMPO-Exp**).

Table 3. Main Results on Pred-Activity. Comparison of SiMPO variants against baselines. Standard SiMPO variants are highlighted in orange, while variants with negative sample awareness are highlighted in blue. The inclusion of negative samples consistently provides the highest gains (+15.2% to +16.9%).

Method	Pred-Activity \uparrow	Improv.
Pretrained	0.17 \pm 0.04	–
CG	3.30 \pm 0.01	–
SMC	4.15 \pm 0.33	–
TDS	4.64 \pm 0.21	–
CFG	5.04 \pm 0.06	–
DRAKES	6.44 \pm 0.04	-1.2%
DRAKES-KL	5.61 \pm 0.07	-13.9%
WD1	3.78 \pm 0.12	-42.0%
RL-D ² (best baseline)	6.52 \pm 0.03	–
SiMPO-Linear	6.54 \pm 0.01	+0.3%
SiMPO-Square	6.77 \pm 0.03	+3.8%
SiMPO-Lin. Neg.	7.51 \pm 0.08	+15.2%
SiMPO-Sqr. Neg.	7.62 \pm 0.08	+16.9%

Results. Our experimental results, summarized in Table 3, demonstrate that **SiMPO** significantly outperforms all considered baselines in terms of the gene expressive levels. While the best-performing baseline, RL-D², achieves a median score of 6.52, our standard linear and square SiMPO variants already provide competitive or superior performance. However, the most substantial gains are observed when incorporating negative sample awareness. Specifically,

²Despite different definitions, discrete diffusion models share most of the properties with continuous diffusion, such as the optimal solution in Equation (3). Please refer to Lou et al. (2023); Shi et al. (2024) for details.

the SiMPO (Ours, Sqr. w/ neg) variant achieves the highest overall performance of 7.62 ± 0.08 , representing a +16.9% improvement over the best baseline. This consistent boost across both linear and square formulations (ranging from +15.2% to +16.9%) suggests that explicitly accounting for negative samples allows the model to better refine diffusion policies, leading to more robust decision-making in complex environments.

5.4. Ablation Studies and Sensitivity Analysis

Ablation on the kl divergence constraint. We test different KL constraint to auto-tune λ (details can be found in Appendix G) with different KL divergence 1.0, 1.5 and 2.0 (upper bound is around 3.47). The results in Figure 6 shows that **SiMPO** is rather robust to KL divergence constraints, and we use 1.5 for all the experiments.

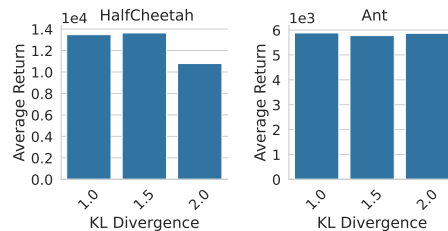


Figure 6. Ablation studies on temperature autotuning with different KL divergence.

6. Conclusions

In this work, we introduced Signed Measure Policy Optimization (SiMPO), a unified framework that generalizes reweighting in diffusion RL through the lens of f -divergence on signed measures. By decomposing the optimization into target measure construction and projection, we revealed that relaxing the non-negativity constraint allows algorithms to actively leverage feedback from negative samples. We provide theoretical justification that negative weights induce a repulsive effect in the velocity field, effectively steering the policy away from suboptimal regions.

Our extensive empirical evaluation, covering bandit problems, MuJoCo locomotion, and DNA sequence generation, demonstrates that SiMPO not only subsumes existing methods like AWR and QVPO but also significantly outperforms them by leveraging flexible, negative-aware reweighting schemes. We hope this paper will inspire more efficient and effective post-training algorithms for diffusion models and flow models.

Impact Statements

This paper presents work whose goal is to advance the field of machine learning. There are many potential societal consequences of our work, none of which we feel must be specifically highlighted here.

References

- Abdolmaleki, A., Springenberg, J. T., Tassa, Y., Munos, R., Heess, N., and Riedmiller, M. Maximum a posteriori policy optimisation. *arXiv preprint arXiv:1806.06920*, 2018.
- Akhound-Sadegh, T., Rector-Brooks, J., Bose, A. J., Mittal, S., Lemos, P., Liu, C.-H., Sendera, M., Ravanbakhsh, S., Gidel, G., Bengio, Y., et al. Iterated denoising energy matching for sampling from boltzmann densities. *arXiv preprint arXiv:2402.06121*, 2024.
- Ali, S. M. and Silvey, S. D. A general class of coefficients of divergence of one distribution from another. *Journal of the Royal Statistical Society: Series B (Methodological)*, 28(1):131–142, 1966.
- Avsec, Ž., Agarwal, V., Visentin, D., Ledsam, J. R., Grabska-Barwinska, A., Taylor, K. R., Assael, Y., Jumper, J., Kohli, P., and Kelley, D. R. Effective gene expression prediction from sequence by integrating long-range interactions. *Nature methods*, 18(10):1196–1203, 2021.
- Black, K., Janner, M., Du, Y., Kostrikov, I., and Levine, S. Training diffusion models with reinforcement learning. *arXiv preprint arXiv:2305.13301*, 2023.
- Broniatowski, M. and Keziou, A. Minimization of φ -divergences on sets of signed measures. *Studia Scientiarum Mathematicarum Hungarica*, 43(4):403–442, 2006.
- Celik, O., Li, Z., Blessing, D., Li, G., Palanicek, D., Peters, J., Chalvatzaki, G., and Neumann, G. Dime: Diffusion-based maximum entropy reinforcement learning. *arXiv preprint arXiv:2502.02316*, 2025.
- Clark, K., Vicol, P., Swersky, K., and Fleet, D. J. Directly fine-tuning diffusion models on differentiable rewards. *arXiv preprint arXiv:2309.17400*, 2023.
- Csiszár, I. and Shields, P. C. Information theory and statistics: A tutorial. 2004.
- Csiszár, I., Gamgoa, F., and Gassiat, E. Mem pixel correlated solutions for generalized moment and interpolation problems. *IEEE Transactions on Information Theory*, 45(7):2253–2270, 2002.
- Ding, S., Hu, K., Zhang, Z., Ren, K., Zhang, W., Yu, J., Wang, J., and Shi, Y. Diffusion-based reinforcement learning via q-weighted variational policy optimization. *arXiv preprint arXiv:2405.16173*, 2024.
- Ding, S., Hu, K., Zhong, S., Luo, H., Zhang, W., Wang, J., Wang, J., and Shi, Y. Genpo: Generative diffusion models meet on-policy reinforcement learning. *arXiv preprint arXiv:2505.18763*, 2025.
- Dong, X., Cheng, J., and Zhang, X. S. Maximum entropy reinforcement learning with diffusion policy. *arXiv preprint arXiv:2502.11612*, 2025.
- Fan, Y., Watkins, O., Du, Y., Liu, H., Ryu, M., Boutilier, C., Abbeel, P., Ghavamzadeh, M., Lee, K., and Lee, K. Dpok: Reinforcement learning for fine-tuning text-to-image diffusion models. *Advances in Neural Information Processing Systems*, 36:79858–79885, 2023.
- Frans, K., Park, S., Abbeel, P., and Levine, S. Diffusion guidance is a controllable policy improvement operator. *arXiv preprint arXiv:2505.23458*, 2025.
- Fujimoto, S., Hoof, H., and Meger, D. Addressing function approximation error in actor-critic methods. In *International conference on machine learning*, pp. 1587–1596. PMLR, 2018.
- Gao, C.-X., Wu, C., Cao, M., Xiao, C., Yu, Y., and Zhang, Z. Behavior-regularized diffusion policy optimization for offline reinforcement learning. In *Forty-second International Conference on Machine Learning*, 2025.
- Gosai, S. J., Castro, R. I., Fuentes, N., Butts, J. C., Kales, S., Noche, R. R., Mouri, K., Sabeti, P. C., Reilly, S. K., and Tewhey, R. Machine-guided design of synthetic cell type-specific cis-regulatory elements. *bioRxiv*, 2023.
- Haarnoja, T., Zhou, A., Abbeel, P., and Levine, S. Soft actor-critic: Off-policy maximum entropy deep reinforcement learning with a stochastic actor. In *International conference on machine learning*, pp. 1861–1870. PMLR, 2018.
- Ho, J. and Salimans, T. Classifier-free diffusion guidance. *arXiv preprint arXiv:2207.12598*, 2022.
- Ho, J., Jain, A., and Abbeel, P. Denoising Diffusion Probabilistic Models. In *Advances in Neural Information Processing Systems*, volume 33, pp. 6840–6851. Curran Associates, Inc., 2020.
- Lan, G. Policy mirror descent for reinforcement learning: Linear convergence, new sampling complexity, and generalized problem classes. *Mathematical programming*, 198(1):1059–1106, 2023.

- Lei, K., Li, H., Yu, D., Wei, Z., Guo, L., Jiang, Z., Wang, Z., Liang, S., and Xu, H. RL-100: Performant robotic manipulation with real-world reinforcement learning. *arXiv preprint arXiv:2510.14830*, 2025.
- Li, T. and He, K. Back to basics: Let denoising generative models denoise. *arXiv preprint arXiv:2511.13720*, 2025.
- Liese, F. and Vajda, I. On divergences and informations in statistics and information theory. *IEEE Transactions on Information Theory*, 52(10):4394–4412, 2006.
- Lipman, Y., Chen, R. T., Ben-Hamu, H., Nickel, M., and Le, M. Flow matching for generative modeling. *arXiv preprint arXiv:2210.02747*, 2022.
- Liu, J., Liu, G., Liang, J., Li, Y., Liu, J., Wang, X., Wan, P., Zhang, D., and Ouyang, W. Flow-grpo: Training flow matching models via online rl. *arXiv preprint arXiv:2505.05470*, 2025.
- Liu, X., Gong, C., and Liu, Q. Flow straight and fast: Learning to generate and transfer data with rectified flow. *arXiv preprint arXiv:2209.03003*, 2022.
- Lou, A., Meng, C., and Ermon, S. Discrete diffusion modeling by estimating the ratios of the data distribution. *arXiv preprint arXiv:2310.16834*, 2023.
- Lu, C., Chen, H., Chen, J., Su, H., Li, C., and Zhu, J. Contrastive energy prediction for exact energy-guided diffusion sampling in offline reinforcement learning. In *International Conference on Machine Learning*, pp. 22825–22855. PMLR, 2023.
- Ma, H., Chen, T., Wang, K., Li, N., and Dai, B. Efficient online reinforcement learning for diffusion policy. *arXiv preprint arXiv:2502.00361*, 2025a.
- Ma, H., Nabati, O., Rosenberg, A., Dai, B., Lang, O., Szpektor, I., Boutilier, C., Li, N., Mannor, S., Shani, L., et al. Reinforcement learning with discrete diffusion policies for combinatorial action spaces. *arXiv preprint arXiv:2509.22963*, 2025b.
- Mei, J., Xiao, C., Dai, B., Li, L., Szepesvári, C., and Schuurmans, D. Escaping the gravitational pull of softmax. *Advances in Neural Information Processing Systems*, 33: 21130–21140, 2020.
- Nair, A., Gupta, A., Dalal, M., and Levine, S. Awac: Accelerating online reinforcement learning with offline datasets. *arXiv preprint arXiv:2006.09359*, 2020.
- Nisonoff, H., Xiong, J., Allenspach, S., and Listgarten, J. Unlocking guidance for discrete state-space diffusion and flow models. *arXiv preprint arXiv:2406.01572*, 2024.
- Peng, X. B., Kumar, A., Zhang, G., and Levine, S. Advantage-weighted regression: Simple and scalable off-policy reinforcement learning. *arXiv preprint arXiv:1910.00177*, 2019.
- Peters, J., Mulling, K., and Altun, Y. Relative entropy policy search. In *Proceedings of the AAAI Conference on Artificial Intelligence*, volume 24, pp. 1607–1612, 2010.
- Physical Intelligence, Amin, A., Aniceto, R., Balakrishna, A., Black, K., Conley, K., Connors, G., Darpinian, J., Dhabalia, K., DiCarlo, J., et al. $\pi_{0.6}^*$: a v1a that learns from experience. *arXiv preprint arXiv:2511.14759*, 2025.
- Prabhudesai, M., Mendonca, R., Qin, Z., Fragkiadaki, K., and Pathak, D. Video diffusion alignment via reward gradients. *arXiv preprint arXiv:2407.08737*, 2024.
- Psenka, M., Escontrela, A., Abbeel, P., and Ma, Y. Learning a diffusion model policy from rewards via q-score matching. *arXiv preprint arXiv:2312.11752*, 2023.
- Puterman, M. L. *Markov decision processes: discrete stochastic dynamic programming*. John Wiley & Sons, 2014.
- Rafailov, R., Sharma, A., Mitchell, E., Manning, C. D., Ermon, S., and Finn, C. Direct preference optimization: Your language model is secretly a reward model. *Advances in neural information processing systems*, 36: 53728–53741, 2023.
- Ren, A. Z., Lidard, J., Ankile, L. L., Simeonov, A., Agrawal, P., Majumdar, A., Burchfiel, B., Dai, H., and Simchowitz, M. Diffusion policy optimization. *arXiv preprint arXiv:2409.00588*, 2024.
- Schulman, J. Trust region policy optimization. *arXiv preprint arXiv:1502.05477*, 2015.
- Schulman, J., Wolski, F., Dhariwal, P., Radford, A., and Klimov, O. Proximal policy optimization algorithms. *arXiv preprint arXiv:1707.06347*, 2017.
- Shani, L., Efroni, Y., and Mannor, S. Adaptive trust region policy optimization: Global convergence and faster rates for regularized mdps. In *Proceedings of the AAAI conference on artificial intelligence*, volume 34, pp. 5668–5675, 2020.
- Shi, J., Han, K., Wang, Z., Doucet, A., and Titsias, M. Simplified and generalized masked diffusion for discrete data. *Advances in neural information processing systems*, 37:103131–103167, 2024.
- Siegel, N. Y., Springenberg, J. T., Berkenkamp, F., Abdolmaleki, A., Neunert, M., Lampe, T., Hafner, R., Heess, N., and Riedmiller, M. Keep doing what worked: Behavioral modelling priors for offline reinforcement learning. *arXiv preprint arXiv:2002.08396*, 2020.

- Song, Y. and Ermon, S. Generative modeling by estimating gradients of the data distribution. *Advances in neural information processing systems*, 32, 2019.
- Tang, X., Dolga, R., Yoon, S., and Bogunovic, I. wd1: Weighted policy optimization for reasoning in diffusion language models. *arXiv preprint arXiv:2507.08838*, 2025.
- Tassa, Y., Doron, Y., Muldal, A., Erez, T., Li, Y., Casas, D. d. L., Budden, D., Abdolmaleki, A., Merel, J., Lefrancq, A., et al. Deepmind control suite. *arXiv preprint arXiv:1801.00690*, 2018.
- Tomar, M., Shani, L., Efroni, Y., and Ghavamzadeh, M. Mirror descent policy optimization, 2021. URL <https://arxiv.org/abs/2005.09814>.
- Vieillard, N., Kozuno, T., Scherrer, B., Pietquin, O., Munos, R., and Geist, M. Leverage the average: an analysis of kl regularization in rl. *arXiv preprint arXiv:2003.14089*, 2020.
- Wang, C., Uehara, M., He, Y., Wang, A., Biancalani, T., Lal, A., Jaakkola, T., Levine, S., Wang, H., and Regev, A. Fine-tuning discrete diffusion models via reward optimization with applications to dna and protein design. *arXiv preprint arXiv:2410.13643*, 2024a.
- Wang, Q., Xiong, J., Han, L., Liu, H., Zhang, T., et al. Exponentially weighted imitation learning for batched historical data. *Advances in Neural Information Processing Systems*, 31, 2018.
- Wang, Y., Wang, L., Jiang, Y., Zou, W., Liu, T., Song, X., Wang, W., Xiao, L., Wu, J., Duan, J., and Li, S. E. Diffusion Actor-Critic with Entropy Regulator, December 2024b.
- Wang, Z., Hunt, J. J., and Zhou, M. Diffusion policies as an expressive policy class for offline reinforcement learning. *arXiv preprint arXiv:2208.06193*, 2022.
- Wu, L., Trippe, B., Naesseth, C., Blei, D., and Cunningham, J. P. Practical and asymptotically exact conditional sampling in diffusion models. *Advances in Neural Information Processing Systems*, 36:31372–31403, 2023.
- Xu, H., Jiang, L., Li, J., Yang, Z., Wang, Z., Chan, V. W. K., and Zhan, X. Offline rl with no ood actions: In-sample learning via implicit value regularization. *arXiv preprint arXiv:2303.15810*, 2023.
- Xu, H., Mao, L., Jin, H., Zhang, W., Zhan, X., and Zhang, A. Uni-rl: Unifying online and offline rl via implicit value regularization. In *The Thirty-ninth Annual Conference on Neural Information Processing Systems*, 2025.
- Yang, L., Huang, Z., Lei, F., Zhong, Y., Yang, Y., Fang, C., Wen, S., Zhou, B., and Lin, Z. Policy representation via diffusion probability model for reinforcement learning. *arXiv preprint arXiv:2305.13122*, 2023.
- Zhang, S., Zhang, W., and Gu, Q. Energy-weighted flow matching for offline reinforcement learning. *arXiv preprint arXiv:2503.04975*, 2025a.
- Zhang, T., Yu, C., Su, S., and Wang, Y. Reinflow: Fine-tuning flow matching policy with online reinforcement learning. *arXiv preprint arXiv:2505.22094*, 2025b.
- Zhang, Y., Yu, S., Zhang, T., Guang, M., Hui, H., Long, K., Wang, Y., Yu, C., and Ding, W. Sac flow: Sample-efficient reinforcement learning of flow-based policies via velocity-reparameterized sequential modeling. *arXiv preprint arXiv:2509.25756*, 2025c.
- Zheng, K., Chen, H., Ye, H., Wang, H., Zhang, Q., Jiang, K., Su, H., Ermon, S., Zhu, J., and Liu, M.-Y. Diffusion-rl: Online diffusion reinforcement with forward process. *arXiv preprint arXiv:2509.16117*, 2025.

A. Related works

RL for diffusion and flow models. RL for diffusion or flow models can be classified into two categories: **a)** Only working with the reverse process, either by computing *policy gradient* via accumulating the log probabilities over the diffusion timesteps (Black et al., 2023; Fan et al., 2023; Ren et al., 2024; Liu et al., 2025; Zhang et al., 2025b), or directly backpropagating gradients through the reverse process by *reparameterization* (Clark et al., 2023; Wang et al., 2024b; Prabhudesai et al., 2024; Celik et al., 2025; Ding et al., 2025; Zhang et al., 2025c; Gao et al., 2025). Such methods closely resemble standard RL algorithms, such as Proximal Policy Optimization (PPO) (Schulman et al., 2017) and Soft Actor Critic (SAC) (Haarnoja et al., 2018), respectively. However, their computational cost typically scales linearly with the number of reverse diffusion steps (Wang et al., 2022; Gao et al., 2025). Moreover, they require a training pipeline that is substantially different from standard score or flow matching, as we need to generate and differentiate through the denoising trajectory. **b)** Another way is preserving the forward process, and steering the score or flow prediction through *weighted behavior cloning* (Ding et al., 2024; Ma et al., 2025a; Zhang et al., 2025a; Tang et al., 2025; Dong et al., 2025) or *moving towards calibrated targets* (Lu et al., 2023; Psenka et al., 2023; Frans et al., 2025; Akhound-Sadegh et al., 2024). In this way, the optimization is well-formulated as distribution matching. In this paper, we dive into the weighted flow matching formula and explore more reweighting options.

Regularizations in policy extraction. KL divergence is widely adopted to regularize the policy regularization and improvement (Peng et al., 2019; Vieillard et al., 2020; Nair et al., 2020). However, it is also possible to adopt other types of divergence metrics. Several works also consider reverse KL regularization (Xu et al., 2025; Ma et al., 2025b), leading to update rules similar to policy gradient theorems. Xu et al. (2023; 2025) further study implicit value regularization, which derives closed-form target policies and update rules for general f -divergence regularized problems. In this paper, we deepen this understanding by extending it to signed measures, thus allowing more flexible and effective objective design. Finally, another branch of research about policy mirror descent is motivated by the Bregman divergence (Tomar et al., 2021; Shani et al., 2020). Notably, the KL divergence occupies a special position, as it is both a Bregman divergence and an f -divergence.

Leveraging negative samples in RL for diffusion models. Negative weights are typically underutilized in weighted behavior cloning and best-of-N distillation. To better exploit such samples in diffusion models, Frans et al. (2025); Physical Intelligence et al. (2025); Zheng et al. (2025) used reward or advantage functions to classify data into preference pairs, and reinforced the diffusion model with classifier-free guidance. Tang et al. (2025) leveraged a weighted behavior cloning with negative weights for diffusion language model reasoning. However, the negative reweighting function is an ad-hoc design, while we provide a generalized and unified viewpoint with theoretical justification.

B. f -divergence on Signed measure.

Let Q be a finite nonnegative measure (e.g., a probability measure) and let P be a finite signed measure. Assume the total variation of P is absolutely continuous with respect to Q , i.e., $|P| \ll Q$, so that the Radon–Nikodym derivative $r := dP/dQ$ exists Q -a.e. and may take negative values. If f is extended to a measurable function on \mathbb{R} (or at least on the essential range of r) such that $f(r) \in L^1(Q)$, we define

$$D_f(P\|Q) := \int f\left(\frac{dP}{dQ}\right) dQ.$$

Moreover, if Q is a probability measure, $P(\Omega) = Q(\Omega) = 1$, and the extension of f is convex on \mathbb{R} with $f(1) = 0$, then Jensen’s inequality yields $D_f(P\|Q) \geq 0$ despite r potentially being negative; under strict convexity, the usual identity-of-indiscernibles conclusion $D_f(P\|Q) = 0 \Rightarrow P = Q$ follows (up to standard regularity/equality conditions).

C. Derivations

C.1. Derivation of the f -Divergence Regularized Policy Optimization

We omit the state s in the following derivation for brevity. Let $f : \mathbb{R}^+ \rightarrow \mathbb{R}$ be strictly convex and differentiable and $f(1) = 0$. We want to find a policy $\pi \in \Pi$ that maximizes the value $Q(\mathbf{a})$ while controlling the f -divergence from the

behavior policy π_{old} , which can be formulated as the following constrained optimization problem:

$$\begin{aligned} & \max_{\pi \in \Pi} \sum_{\mathbf{a} \in \mathcal{A}} \pi(\mathbf{a})Q(\mathbf{a}) \\ & \text{s.t.} \begin{cases} D_f(\pi(\cdot) \parallel \pi_{\text{old}}(\cdot)) \leq \epsilon \\ \sum_{\mathbf{a} \in \mathcal{A}} \pi(\mathbf{a}) = 1 \\ \forall \mathbf{a} \in \mathcal{A}, \pi(\mathbf{a}) \geq 0 \end{cases} \end{aligned} \quad (12)$$

We introduce Lagrange multipliers λ , ν , and $\eta(\mathbf{a}) \geq 0$ for the constraints, respectively, leading to the following Lagrange function \mathcal{L} ,

$$\mathcal{L}(\pi, \lambda, \nu, \eta) = \sum_{\mathbf{a} \in \mathcal{A}} \pi(\mathbf{a})Q(\mathbf{a}) - \lambda \left(\sum_{\mathbf{a} \in \mathcal{A}} \pi_{\text{old}}(\mathbf{a})f\left(\frac{\pi(\mathbf{a})}{\pi_{\text{old}}(\mathbf{a})}\right) - \epsilon \right) - \nu(1 - \sum_{\mathbf{a} \in \mathcal{A}} \pi(\mathbf{a})) + \sum_{\mathbf{a} \in \mathcal{A}} \eta(\mathbf{a})\pi(\mathbf{a}). \quad (13)$$

We take the functional derivative with respect to $\pi(\mathbf{a})$ and set it to zero. Recall that the derivative of the term $\mu f(\pi/\mu)$ with respect to π is $f'(\pi/\mu)$,

$$0 = \frac{\partial \mathcal{L}}{\partial \pi(\mathbf{a})} = Q(\mathbf{a}) - \lambda f'\left(\frac{\pi(\mathbf{a})}{\pi_{\text{old}}(\mathbf{a})}\right) - \nu + \eta(\mathbf{a}), \quad (14)$$

Rearranging to isolate the divergence term,

$$f'\left(\frac{\pi(\mathbf{a})}{\pi_{\text{old}}(\mathbf{a})}\right) = \frac{Q(\mathbf{a}) - \nu + \eta(\mathbf{a})}{\lambda}. \quad (15)$$

We define $g_f = (f')^{-1}$. Since the complimentary slackness requires $\eta(\mathbf{a})\pi(\mathbf{a}) = 0$, we consider the following cases:

- $\pi(\mathbf{a}) > 0$, in this case $\eta(\mathbf{a}) = 0$, therefore we have

$$f'\left(\frac{\pi(\mathbf{a})}{\pi_{\text{old}}(\mathbf{a})}\right) = \frac{Q(\mathbf{a}) - \nu}{\lambda} \Rightarrow \frac{\pi(\mathbf{a})}{\pi_{\text{old}}(\mathbf{a})} = g_f\left(\frac{Q(\mathbf{a}) - \nu}{\lambda}\right)$$

Besides, since f is strongly convex, both f' and g_f are increasing, therefore

$$\frac{Q(\mathbf{a}) - \nu}{\lambda} = f'\left(\frac{\pi(\mathbf{a})}{\pi_{\text{old}}(\mathbf{a})}\right) > f'(0).$$

- $\pi(\mathbf{a}) = 0$, in this case $\eta(\mathbf{a}) > 0$. From the stationary condition, we know that

$$Q(\mathbf{a}) - \nu + \eta(\mathbf{a}) = \lambda f'(0) \Rightarrow \frac{Q(\mathbf{a}) - \nu}{\lambda} < f'(0).$$

Therefore, for both cases, we can unify the optimal solution as

$$\pi(\mathbf{a}) = \pi_{\text{old}}(\mathbf{a})\bar{g}_f\left(\frac{Q(\mathbf{a}) - \nu}{\lambda}\right), \quad (16)$$

where

$$\bar{g}_f(x) = \begin{cases} g_f(x) & \text{if } x > f'(0) \\ 0 & \text{if } x \leq f'(0) \end{cases}. \quad (17)$$

C.2. Derivation of the f -Divergence Regularized Policy Optimization on Signed Measures

Let $f(x) : \mathbb{R} \rightarrow \mathbb{R}$ be strictly convex and differentiable and $f(1) = 0$. Since f is strictly convex, f' is monotonically increasing, and therefore $g_f = (f')^{-1}$ is well defined. Consider the solution space $\tilde{\Pi} = \{\pi : \sum_{\mathbf{a} \sim \mathcal{A}} \pi(\mathbf{a}) = 1\}$, the optimization problem regularized the generalized f -divergence is defined as

$$\begin{aligned} & \max_{\pi \in \tilde{\Pi}} \sum_{\mathbf{a} \in \mathcal{A}} \pi(\mathbf{a})Q(\mathbf{a}) \\ & \text{s.t.} \begin{cases} D_f(\pi(\cdot) \parallel \pi_{\text{old}}(\cdot)) \leq \epsilon \\ \sum_{\mathbf{a} \in \mathcal{A}} \pi(\mathbf{a}) = 1 \end{cases} \end{aligned} \quad (18)$$

We introduce Lagrange multipliers λ and ν for the constraints, leading to the following Lagrange function \mathcal{L} :

$$\mathcal{L}(\pi, \lambda, \nu) = \sum_{\mathbf{a} \in \mathcal{A}} \pi(\mathbf{a})Q(\mathbf{a}) - \lambda \left(\sum_{\mathbf{a} \in \mathcal{A}} \pi_{\text{old}}(\mathbf{a})f \left(\frac{\pi(\mathbf{a})}{\pi_{\text{old}}(\mathbf{a})} \right) - \epsilon \right) - \nu \left(1 - \sum_{\mathbf{a} \in \mathcal{A}} \pi(\mathbf{a}) \right). \quad (19)$$

Taking its derivative w.r.t. $\pi(\mathbf{a})$ and setting it to zero:

$$0 = \frac{\partial \mathcal{L}}{\partial \pi(\mathbf{a})} = Q(\mathbf{a}) - \lambda f' \left(\frac{\pi(\mathbf{a})}{\pi_{\text{old}}(\mathbf{a})} \right) - \nu, \quad (20)$$

i.e.,

$$\pi(\mathbf{a}) = \pi_{\text{old}}(\mathbf{a})(f')^{-1} \left(\frac{Q(\mathbf{a}) - \nu}{\lambda} \right) = \pi_{\text{old}}(\mathbf{a})g_f \left(\frac{Q(\mathbf{a}) - \nu}{\lambda} \right).$$

Note that ν is the normalization term such that $\sum_{\mathbf{a} \in \mathcal{A}} \mu(\mathbf{a})g((Q(\mathbf{a}) - \nu)/\lambda) = 1$.

Generally speaking, for any strictly increasing (and typically continuous) function g defined on an interval $I \subseteq \mathbb{R}$, its inverse g^{-1} exists on $g(I)$ and is strictly increasing. Define $f_g(x) = g^{-1}(x)$ for $x \in g(I)$ and

$$f_g(x) = \int_{a_0}^x g^{-1}(t)dt + C$$

yields a differentiable strictly convex function on $g(I)$. Normalizing $f_g(1) = 0$ underpins C . While the analytic formulation of f_g may not be available for an arbitrary g , this observation allows us to reason directly in terms of the weighting function g rather than f_g .

C.3. Policy Improvement Property of the Target Measure

Theorem C.1 (Theorem 3.5 restated). *Assume $g : \mathbb{R} \rightarrow \mathbb{R}$ is monotonic increasing and the target measure $\tilde{\pi}$ is defined as*

$$\tilde{\pi}(\mathbf{a}|\mathbf{s}) = \pi(\mathbf{a}|\mathbf{s})g \left(\frac{Q(\mathbf{s}, \mathbf{a}) - \nu}{\lambda} \right) \quad \forall \mathbf{s} \in \mathcal{S},$$

where $\lambda > 0$ and ν is selected such that $\sum_{\mathbf{a} \in \mathcal{A}} \tilde{\pi}(\mathbf{a}|\mathbf{s}) = 1$ holds. Then we have

$$\sum_{\mathbf{a} \in \mathcal{A}} \tilde{\pi}(\mathbf{a}|\mathbf{s})Q(\mathbf{s}, \mathbf{a}) \geq \sum_{\mathbf{a} \in \mathcal{A}} \pi(\mathbf{a}|\mathbf{s})Q(\mathbf{s}, \mathbf{a}) \quad \forall \mathbf{s} \in \mathcal{S}.$$

Proof. Denote $A(\mathbf{s}, \mathbf{a}) = \frac{Q(\mathbf{s}, \mathbf{a}) - \nu}{\lambda}$, and thus we have $\sum_{\mathbf{a} \in \mathcal{A}} \tilde{\pi}(\mathbf{a}|\mathbf{s}) = \mathbb{E}_{\pi}[g(A(\mathbf{s}, \mathbf{a}))] = 1$. It suffices to show

$$\sum_{\mathbf{a} \in \mathcal{A}} \tilde{\pi}(\mathbf{a}|\mathbf{s})A(\mathbf{s}, \mathbf{a}) \geq \sum_{\mathbf{a} \in \mathcal{A}} \pi(\mathbf{a}|\mathbf{s})A(\mathbf{s}, \mathbf{a}).$$

Consider the difference

$$\begin{aligned} & \sum_{\mathbf{a} \in \mathcal{A}} \tilde{\pi}(\mathbf{a}|\mathbf{s})A(\mathbf{s}, \mathbf{a}) - \sum_{\mathbf{a} \in \mathcal{A}} \pi(\mathbf{a}|\mathbf{s})A(\mathbf{s}, \mathbf{a}) \\ &= \sum_{\mathbf{a} \in \mathcal{A}} \pi(\mathbf{a}|\mathbf{s})A(\mathbf{s}, \mathbf{a})g(A(\mathbf{s}, \mathbf{a})) - \left(\sum_{\mathbf{a} \in \mathcal{A}} \pi(\mathbf{a}|\mathbf{s})A(\mathbf{s}, \mathbf{a}) \right) \left(\sum_{\mathbf{a} \in \mathcal{A}} \pi(\mathbf{a}|\mathbf{s})g(A(\mathbf{s}, \mathbf{a})) \right) \\ &= \mathbb{E}_{\pi}[A(\mathbf{s}, \mathbf{a})g(A(\mathbf{s}, \mathbf{a}))] - \mathbb{E}_{\pi}[A(\mathbf{s}, \mathbf{a})]\mathbb{E}_{\pi}[g(A(\mathbf{s}, \mathbf{a}))] \\ &= \text{Cov}_{\pi}[A(\mathbf{s}, \mathbf{a}), g(A(\mathbf{s}, \mathbf{a}))]. \end{aligned}$$

Since g is monotonic increasing, we know that $\text{Cov}_{\pi}[A(\mathbf{s}, \mathbf{a}), g(A(\mathbf{s}, \mathbf{a}))] \geq 0$, and thus

$$\sum_{\mathbf{a} \in \mathcal{A}} \tilde{\pi}(\mathbf{a}|\mathbf{s})A(\mathbf{s}, \mathbf{a}) \geq \sum_{\mathbf{a} \in \mathcal{A}} \pi(\mathbf{a}|\mathbf{s})A(\mathbf{s}, \mathbf{a}).$$

□

D. Derivation of Closed-Form Solution of Reweighted Conditional Flow Matching.

Notation. We temporarily omit conditioning on the state \mathbf{s} for clarity.

D.1. Closed-Form Solution of Conditional Flow Matching.

To warm up, we first show the optimal solution of flow matching when there is no reweighting factor $w(\mathbf{a})$:

Lemma D.1 (Conditional flow matching fits marginal velocity (Lipman et al., 2022)). *The Conditional Flow Matching loss*

function is defined as:

$$\mathcal{L}_{\text{CFM}}(\theta) = \mathbb{E}_{t \sim \mathcal{U}[0,1], \mathbf{a}_0 \sim \pi_{\text{old}}(\mathbf{a}_0), \mathbf{a}_t \sim p_t(\cdot | \mathbf{a}_0)} [\|D_\theta(\mathbf{a}_t; t) - \mathbf{v}_t(\mathbf{a}_t | \mathbf{a}_0)\|^2]$$

Proof. To find the minimum, we look for the vector field $v(x)$ that minimizes the objective at any specific point in space and time.

Step 1: Rewrite the Expectation. We expand the expectation integrals over the joint distribution of data \mathbf{a}_0 and intermediate samples x .

$$\mathcal{L} = \int_0^1 \int \int \pi_{\text{old}}(\mathbf{a}_0) p_{t|0}(\mathbf{a} | \mathbf{a}_0) \|D_\theta(\mathbf{a}_t; t) - \mathbf{v}_t(\mathbf{a}_t | \mathbf{a}_0)\|^2 d\mathbf{a}_0 d\mathbf{a}_t dt$$

Step 2: Apply Bayes' Rule. We can decompose the joint distribution $\pi_{\text{old}}(\mathbf{a}_0) p_{t|0}(\mathbf{a} | \mathbf{a}_0)$ in the reverse direction using the marginal $p_t(\mathbf{a}_t)$ and the posterior $p_{0|t}(\mathbf{a}_0 | \mathbf{a}_t)$:

$$\pi_{\text{old}}(\mathbf{a}_0) p_{t|0}(\mathbf{a}_t | \mathbf{a}_0) = p_t(\mathbf{a}_t) p_{0|t}(\mathbf{a}_0 | \mathbf{a}_t)$$

Substitute this into the loss integral:

$$\mathcal{L} = \int_0^1 \int p_t(\mathbf{a}_t) \left[\int p_{0|t}(\mathbf{a}_0 | \mathbf{a}_t) \|D_\theta(\mathbf{a}_t; t) - \mathbf{v}_t(\mathbf{a}_t | \mathbf{a}_0)\|^2 d\mathbf{a}_0 \right] d\mathbf{a}_t dt$$

Step 3: Pointwise Minimization. Since $p_t(\mathbf{a}_t)$ and dt are non-negative, minimizing the total integral is equivalent to minimizing the inner term (the term in square brackets) for every specific location \mathbf{a}_t and time t . Define the local objective $J(v)$ for a fixed \mathbf{a}_t and t :

$$J(v) = \int p_{0|t}(\mathbf{a}_0 | \mathbf{a}_t) \|v - \mathbf{v}_t(\mathbf{a}_t | \mathbf{a}_0)\|^2 d\mathbf{a}_0$$

This is a standard Least Squares problem. We are looking for a constant vector v (constant with respect to \mathbf{a}_0) that minimizes the expected squared distance to the random variable $\mathbf{v}_t(\mathbf{a}_t | \mathbf{a}_0)$.

Step 4: Solve for v . We take the gradient of $J(v)$ with respect to v and set it to zero:

$$\nabla_v J(v) = \int p_{0|t}(\mathbf{a}_0 | \mathbf{a}_t) \cdot 2(v - \mathbf{v}_t(\mathbf{a}_t | \mathbf{a}_0)) d\mathbf{a}_0 = 0$$

$$\int p_{0|t}(\mathbf{a}_0 | \mathbf{a}_t) v d\mathbf{a}_0 = \int p_{0|t}(\mathbf{a}_0 | \mathbf{a}_t) \mathbf{v}_t(\mathbf{a}_t | \mathbf{a}_0) d\mathbf{a}_0$$

Since v does not depend on \mathbf{a}_0 , we pull it out of the integral. Note that $\int p_{0|t}(\mathbf{a}_0 | \mathbf{a}_t) d\mathbf{a}_0 = 1$:

$$v \cdot 1 = \int \mathbf{v}_t(\mathbf{a}_t | \mathbf{a}_0) p_{0|t}(\mathbf{a}_0 | \mathbf{a}_t) d\mathbf{a}_0$$

$$v^* = \mathbb{E}_{\mathbf{a}_0 \sim p_{0|t}(\mathbf{a}_0 | \mathbf{a}_t)} [\mathbf{v}_t(\mathbf{a}_t | \mathbf{a}_0)]$$

Finally, by definition, we know that the marginal velocity field $\mathbf{u}_t(\mathbf{x}_t)$ is defined exactly by

$$\mathbf{u}_t \doteq \mathbb{E}_{\mathbf{a}_0 \sim p_{0|t}(\mathbf{a}_0 | \mathbf{a}_t)} [\mathbf{v}_t(\mathbf{a}_t | \mathbf{a}_0)] = v^*,$$

which concludes the proof. \square

Corollary D.2 (Diffusion marginal velocity field is the noisy score functions.). *Specifically, for the VE diffusion models, the marginal velocity field is the score function of the perturbed data distribution, i.e.,*

$$\mathbf{u}_t(\mathbf{a}_t) = \nabla_{\mathbf{a}_t} \log D_\theta(\mathbf{a}_t; t)$$

which is derived by

$$\begin{aligned} \mathbf{u}_t &\doteq \mathbb{E}_{\mathbf{a}_0 \sim p_{0|t}(\mathbf{a}_0 | \mathbf{a}_t)} [\mathbf{v}_t(\mathbf{a}_t | \mathbf{a}_0)] = \int p_{0|t}(\mathbf{a}_0 | \mathbf{a}_t) \nabla \log p_{t|0}(\mathbf{a}_t | \mathbf{a}_0) d\mathbf{a}_0 \\ &= \int \frac{p_{t|0}(\mathbf{a}_t | \mathbf{a}_0) \pi_{\text{old}}(\mathbf{a}_0)}{p_t(\mathbf{a}_t)} \nabla \log p_{t|0}(\mathbf{a}_t | \mathbf{a}_0) d\mathbf{a}_0 = \frac{1}{p_t(\mathbf{a}_t)} \int \pi_{\text{old}}(\mathbf{a}_0) \nabla p_{t|0}(\mathbf{a}_t | \mathbf{a}_0) d\mathbf{a}_0 = \frac{1}{p_t(\mathbf{a}_t)} \nabla p_t(\mathbf{a}_t) = \nabla \log p_t(\mathbf{a}_t) \end{aligned}$$

D.2. Closed-Form Solution of Reweighted Conditional Flow Matching.

Then we show our main results about the reweighted conditional flow matching

Theorem D.3 (Optimal solution of the reweighted conditional flow matching.). *When $\mathbb{E}_{\mathbf{a}_0 \sim p_{0|t}} [w(\mathbf{a}_0)] > 0$, the reweighted conditional flow matching loss*

$$\mathcal{L}_W = \mathbb{E}_{t \sim \mathcal{U}, \mathbf{a}_0 \sim \pi_{\text{old}}(\mathbf{a}_0), x \sim p_{t|0}(\mathbf{a} | \mathbf{a}_0)} [w(\mathbf{a}_0) \|D_\theta(\mathbf{a}_t; t) - \mathbf{v}_t(\mathbf{a}_t | \mathbf{a}_0)\|^2]$$

induces optimal solution

$$v_t^*(\mathbf{a}_t; t) = \frac{\mathbb{E}_{\mathbf{a}_0 \sim p_{0|t}}[w(\mathbf{a}_0)\mathbf{v}_t(\mathbf{a}_t|\mathbf{a}_0)]}{\mathbb{E}_{\mathbf{a}_0 \sim p_{0|t}}[w(\mathbf{a}_0)]}$$

Step 1: Rewrite as an Integral.

Expand the expectations into their integral forms:

$$\mathcal{L}_W = \int_0^1 \int \int \pi_{\text{old}}(\mathbf{a}_0)p_{t|0}(\mathbf{a}|\mathbf{a}_0)w(\mathbf{a}_0)\|D_\theta(\mathbf{a}_t; t) - \mathbf{v}_t(\mathbf{a}_t|\mathbf{a}_0)\|^2 d\mathbf{a}_0 d\mathbf{a}_t dt$$

Step 2: Apply Bayes' Rule.

Substitute the joint distribution $\pi_{\text{old}}(\mathbf{a}_0)p_{t|0}(\mathbf{a}|\mathbf{a}_0)$ with the marginal-posterior decomposition $p_t(\mathbf{a}_t)p_{0|t}(\mathbf{a}_0|\mathbf{a}_t)$. Note that $w(\mathbf{a}_0)$ remains attached to the inner integral over \mathbf{a}_0 .

$$\mathcal{L}_W = \int_0^1 \int p_t(\mathbf{a}_t) \left[\int p_{0|t}(\mathbf{a}_0|\mathbf{a}_t)w(\mathbf{a}_0)\|D_\theta(\mathbf{a}_t; t) - \mathbf{v}_t(\mathbf{a}_t|\mathbf{a}_0)\|^2 d\mathbf{a}_0 \right] d\mathbf{a}_t dt$$

Step 3: Pointwise Minimization.

To minimize the global loss, we minimize the inner term (in square brackets) for every fixed point x and time t . Let $J_W(v)$ be this local weighted objective:

$$J_W(v) = \int p_{0|t}(\mathbf{a}_0|\mathbf{a}_t)w(\mathbf{a}_0)\|v - \mathbf{v}_t(\mathbf{a}_t|\mathbf{a}_0)\|^2 d\mathbf{a}_0$$

Step 4: Solve for v .

Rewrite the pointwise loss function, we have

$$J_W(v) = \underbrace{\left(\int p_{0|t}(\mathbf{a}_0|\mathbf{a}_t)w(\mathbf{a}_0) d\mathbf{a}_0 \right)}_{M(\mathbf{a}_t)} \|v\|^2 - 2v^T \underbrace{\left(\int p_{0|t}(\mathbf{a}_0|\mathbf{a}_t)w(\mathbf{a}_0)\mathbf{v}_t(\mathbf{a}_t|\mathbf{a}_0) d\mathbf{a}_0 \right)}_{N(\mathbf{a}_t)} + C \quad (21)$$

The closed-form optimal solution only exists when $M(\mathbf{a}_t) > 0$.

Calculate the gradient with respect to v and set it to zero:

$$\nabla_v J_W(v) = \int p_{0|t}(\mathbf{a}_0|\mathbf{a}_t)w(\mathbf{a}_0) \cdot 2(v - \mathbf{v}_t(\mathbf{a}_t|\mathbf{a}_0)) d\mathbf{a}_0 = 0$$

Distribute the terms. Note that v is constant with respect to the integral over \mathbf{a}_0 :

$$v \int p_{0|t}(\mathbf{a}_0|\mathbf{a}_t)w(\mathbf{a}_0) d\mathbf{a}_0 = \int p_{0|t}(\mathbf{a}_0|\mathbf{a}_t)w(\mathbf{a}_0)\mathbf{v}_t(\mathbf{a}_t|\mathbf{a}_0) d\mathbf{a}_0$$

Crucial Difference: In the unweighted case, the integral on the left side was $\int p_{0|t}(\mathbf{a}_0|\mathbf{a}_t)d\mathbf{a}_0 = 1$. Here, the integral is over the weighted posterior, so it does not sum to 1. It acts as a normalizing constant for the weights. We solve for v :

$$v = \frac{\int p_{0|t}(\mathbf{a}_0|\mathbf{a}_t)w(\mathbf{a}_0)\mathbf{v}_t(\mathbf{a}_t|\mathbf{a}_0) d\mathbf{a}_0}{\int p_{0|t}(\mathbf{a}_0|\mathbf{a}_t)w(\mathbf{a}_0) d\mathbf{a}_0}$$

Rearrange it we get the optimal solution,

$$v_t^*(\mathbf{a}_t) = \frac{\mathbb{E}_{\mathbf{a}_0 \sim p_{0|t}}[w(\mathbf{a}_0)\mathbf{v}_t(\mathbf{a}_t|\mathbf{a}_0)]}{\mathbb{E}_{\mathbf{a}_0 \sim p_{0|t}}[w(\mathbf{a}_0)]}$$

D.3. Velocity field generates reweighted data distribution.

We aim to derive

In **Case I** when \mathbf{a}_t satisfies $\mathbb{E}_{\mathbf{a}_0 \sim p_{0|t}(\cdot|\mathbf{a}_t)}[w(\mathbf{s}, \mathbf{a}_0)] > 0$, the closed-form velocity field solution Equation (8) generate probability path

$$\rho_t(\mathbf{a}|\mathbf{s}) = \frac{1}{Z} \int w(\mathbf{s}, \mathbf{a}_0)\pi_{\text{old}}(\mathbf{a}_0|\mathbf{s})p_{t|0}(\mathbf{a}|\mathbf{a}_0) d\mathbf{a}_0$$

where $Z(s)$ is the global normalizing constant: $Z = \int w(s, \mathbf{a}_0) \pi_{\text{old}}(\mathbf{a}_0 | s) d\mathbf{a}_0$.

Proof. To prove $v_t^*(\mathbf{a}; t)$ generates this distribution, we just need to verify that it satisfies the Continuity Equation (Conservation of Mass) for $\rho_t(x)$. The continuity equation states:

$$\frac{\partial \rho_t}{\partial t} + \nabla \cdot (\rho_t v_t^*) = 0$$

Step A: Expand the Divergence Term.

Let's look at the flow term $\rho_t v_t^*$. Substituting your definition of the optimal solution:

$$v_t^*(\mathbf{a}_t) = \frac{\mathbb{E}_{p_{0|t}}[w\mathbf{v}]}{\mathbb{E}_{p_{0|t}}[w]} = \frac{\int w(\mathbf{a}_0) p_{t|0}(\mathbf{a}_t | \mathbf{a}_0) \pi_{\text{old}}(\mathbf{a}_0) \mathbf{v}_t(\mathbf{a}_t | \mathbf{a}_0) d\mathbf{a}_0}{\int w(\mathbf{a}_0) p_{t|0}(\mathbf{a}_t | \mathbf{a}_0) \pi_{\text{old}}(\mathbf{a}_0) d\mathbf{a}_0}$$

The denominator is exactly the unnormalized density, let's call it $\tilde{\rho}_t(x) = Z \rho_t(x)$. So, $\tilde{\rho}_t(x) v_t^*(\mathbf{a}_t)$ is just the numerator:

$$\tilde{\rho}_t v_t^* = \int w(\mathbf{a}_0) \pi_{\text{old}}(\mathbf{a}_0) [p_{t|0}(\mathbf{a}_t | \mathbf{a}_0) \mathbf{v}_t(\mathbf{a}_t | \mathbf{a}_0)] d\mathbf{a}_0$$

Step B: Apply Divergence

$$\nabla \cdot (\tilde{\rho}_t v_t^*) = \int w(\mathbf{a}_0) \pi_{\text{old}}(\mathbf{a}_0) \underbrace{\nabla \cdot (p_{t|0}(\mathbf{a}_t | \mathbf{a}_0) \mathbf{v}_t(\mathbf{a}_t | \mathbf{a}_0))}_{\text{Conditional Continuity}} d\mathbf{a}_0$$

We know that for the conditional path (e.g., Gaussian), the conditional velocity \mathbf{u}_t satisfies continuity: $\nabla \cdot (p\mathbf{u}) = -\frac{\partial p}{\partial t}$. Substitute this back:

$$\nabla \cdot (\tilde{\rho}_t v_t^*) = \int w(\mathbf{a}_0) \pi_{\text{old}}(\mathbf{a}_0) \left(-\frac{\partial p_{t|0}(\mathbf{a}_t | \mathbf{a}_0)}{\partial t} \right) d\mathbf{a}_0$$

Step C: Linearity of the Derivative Pull the derivative and negative sign out:

$$\nabla \cdot (\tilde{\rho}_t v_t^*) = -\frac{\partial}{\partial t} \int w(\mathbf{a}_0) \pi_{\text{old}}(\mathbf{a}_0) p_{t|0}(\mathbf{a}_t | \mathbf{a}_0) d\mathbf{a}_0 = -\frac{\partial \tilde{\rho}_t}{\partial t}$$

Result:

$$\frac{\partial \tilde{\rho}_t}{\partial t} + \nabla \cdot (\tilde{\rho}_t v_t^*) = 0$$

This confirms that the vector field indeed evolves the initial distribution $\rho_0(x)$ to $\rho_1(x)$ according to the laws of probability flow. □

D.4. Cases when $\mathbb{E}_{\mathbf{a}_0 \sim p_{0|t}}[w(\mathbf{a}_0)] \leq 0$.

Corollary D.4. When $\mathbb{E}_{\mathbf{a}_0 \sim p_{0|t}}[w(\mathbf{a}_0)]$, the loss in (21) is unbounded and the gradient push v away from

Proof. the Equation (21) can be rewritten by $M(\mathbf{a}_t) \|v\|^2 - 2N(\mathbf{a}_t)$ □

E. Derivation of Closed-Form Solutions for Linear and Square Weighting

In this section, we derive the closed-form solutions for the scalar v under two common constraints involving the Rectified Linear Unit (ReLU). We consider a batch of samples $\{x_i\}_{i=1}^N$ and a scaling parameter l .

E.1. General Setup and Notation

We sort the samples in descending order such that $x_{(1)} \geq x_{(2)} \geq \dots \geq x_{(N)}$. We define the *active set* S as the set of indices where the ReLU term is non-zero, i.e., $S = \{i \mid x_i > v\}$. Let $k = |S|$ denote the number of active samples. For $i \in S$, $\text{ReLU}(x_i - v) = x_i - v$; otherwise, it is 0.

Because the objective functions in both cases are monotonic with respect to v , we can determine the optimal active set size k efficiently by checking conditions on the sorted samples.

E.2. Case 1: Linear Constraint

We first consider the linear constraint:

$$\frac{1}{N} \sum_{i=1}^N \frac{\text{ReLU}(x_i - v)}{l} = 1. \quad (22)$$

Rearranging, we require the sum of active excesses to equal the target mass $C_1 = N \cdot l$:

$$\sum_{i \in S} (x_i - v) = C_1. \quad (23)$$

Solving for v yields the solution:

$$v = \frac{1}{k} \left(\sum_{i \in S} x_i - C_1 \right). \quad (24)$$

To determine k , we find the largest index k such that the “excess mass” at the boundary $x_{(k)}$ is strictly less than the target C_1 :

$$\sum_{j=1}^k (x_{(j)} - x_{(k)}) < N \cdot l. \quad (25)$$

E.3. Case 2: Squared Constraint

Next, we consider the squared constraint:

$$\frac{1}{N} \sum_{i=1}^N \left(\frac{\text{ReLU}(x_i - v)}{l} \right)^2 = 1. \quad (26)$$

Let $C_2 = N \cdot l^2$. Expanding the square over the active set S , we obtain a quadratic equation in v :

$$\begin{aligned} \sum_{i \in S} (x_i - v)^2 &= C_2 \\ kv^2 - 2 \left(\sum_{i \in S} x_i \right) v + \left(\sum_{i \in S} x_i^2 - C_2 \right) &= 0. \end{aligned} \quad (27)$$

Using the quadratic formula and selecting the negative root (since v acts as a lower cutoff and must satisfy $v < \frac{1}{k} \sum x_i$ to generate variance), we obtain:

$$v = \frac{1}{k} \left(\sum_{i \in S} x_i - \sqrt{\left(\sum_{i \in S} x_i \right)^2 - k \left(\sum_{i \in S} x_i^2 - C_2 \right)} \right). \quad (28)$$

To determine k in this case, we compute the “energy at the boundary” E_k for the candidate cutoff $x_{(k)}$ and select the largest k such that $E_k < C_2$:

$$E_k = \sum_{j=1}^k (x_{(j)} - x_{(k)})^2 < N \cdot l^2. \quad (29)$$

E.4. Reference Implementation

We provide a vectorized JAX implementation for solving both the linear and squared constraints derived in Section E. This implementation supports batch processing and is differentiable.

Listing 1. JAX implementation for solving v .

```
import jax.numpy as jnp

def solve_v(x, l, mode='linear'):
    """
    Solves for v given batch input x and scale l.
    mode: 'linear' for mean(ReLU(x-v)/l) = 1
          'squared' for mean((ReLU(x-v)/l)^2) = 1
    """
    N = x.shape[-1]
```

```

# Sort descending: x_(1) >= x_(2) ...
x_sorted = jnp.sort(x, axis=-1)[: , ::-1]
cumsum_x = jnp.cumsum(x_sorted, axis=-1)
k_indices = jnp.arange(1, N + 1)

if mode == 'linear':
    target = N * l
    # Excess mass at boundary x_(k)
    excess = cumsum_x - k_indices * x_sorted

    # Find largest k where excess < target
    mask = excess < target
    k_star = jnp.sum(mask, axis=-1, keepdims=True)

    # Calculate v
    sum_active = jnp.take_along_axis(cumsum_x, k_star - 1, axis=-1)
    return (sum_active - target) / k_star

elif mode == 'squared':
    C = N * (l ** 2)
    cumsum_x2 = jnp.cumsum(x_sorted ** 2, axis=-1)

    # Energy at boundary x_(k)
    energy = (cumsum_x2 - 2 * x_sorted * cumsum_x
              + k_indices * (x_sorted ** 2))

    # Find largest k where energy < C
    mask = energy < C
    k_star = jnp.maximum(jnp.sum(mask, axis=-1, keepdims=True), 1)

    # Gather active stats
    S1 = jnp.take_along_axis(cumsum_x, k_star - 1, axis=-1)
    S2 = jnp.take_along_axis(cumsum_x2, k_star - 1, axis=-1)

    # Quadratic formula (negative root)
    delta = S1**2 - k_star * (S2 - C)
    return (S1 - jnp.sqrt(jnp.maximum(delta, 0.0))) / k_star

```

F. Experimental Details

F.1. Baselines

We evaluate our approach against two distinct families of reinforcement learning (RL) algorithms. The first group consists of five state-of-the-art **online diffusion-policy methods**, encompassing both off-policy and on-policy architectures:

- **QSM** (Psenka et al., 2023): Implements Langevin dynamics using the gradient of a learned Q -function as the score function.
- **QVPO** (Ding et al., 2024): Employs a Q -weighted variational objective for diffusion training, though it is notably constrained by its inability to process negative rewards effectively.
- **DACER** (Wang et al., 2024b): Backpropagates gradients directly through the reverse diffusion process and utilizes a GMM entropy regulator to manage the exploration-exploitation trade-off.
- **DIPO** (Yang et al., 2023): Uses a two-stage approach where state-action particles are updated via Q -gradients before being fitted to a diffusion model.
- **DPPO** (Ren et al., 2024): Formulates a dual-layer MDP spanning diffusion and environment steps, optimized via Proximal Policy Optimization. We employ the training-from-scratch configuration to maintain a fair comparison with other methods.

The second group includes three **classic model-free baselines**: **PPO** (Schulman et al., 2017), **TD3** (Fujimoto et al., 2018), and **SAC** (Haarnoja et al., 2018). For PPO, we utilize a buffer size of 4096 and perform 10 gradient updates per sample. Across all baselines, we collect samples from 5 parallel environments for a total of 1 million environment interactions and 200k iterations. Performance is reported as the average return over 20 episodes across 5 random seeds.

Table 4. Hyperparameters

Name	Value
Critic learning rate	3e-4
Policy learning rate	3e-4, linear annealing to 3e-5
Diffusion steps	20
Diffusion noise schedules	Cosine
Policy network hidden layers	3
Policy network hidden neurons	256
Policy network activation	Mish
Value network hidden layers	3
Value network hidden neurons	256
Value network activation	Mish
replay buffer size (off-policy only)	1 million

where the Cosine noise schedule means $\beta_t = 1 - \frac{\bar{\alpha}_t}{\alpha_{t-1}}$ with $\bar{\alpha}_t = \frac{f(t)}{f(0)}$, $f(t) = \cos\left(\frac{t/T+s}{1+s} * \frac{\pi}{2}\right)^2$.

To provide a formal mathematical summary of the reward functions for your paper, you can use the following LaTeX code. It uses the amsmath package for aligned equations and a table for comparison.

F.2. Reward Functions

The Cheetah domain tasks are designed to track a target horizontal velocity $v^* = 10.0$ m/s (limited by the physical capability, the robot cannot actually achieve 10m/s. Therefore, the task is to run as fast as possible.). Let v denote the current horizontal velocity of the torso. We evaluate our method across several reward formulations, categorized into linear, quadratic, and absolute value variations.

We design the following reward functions (with proper transformation to align the scale), ranked from “flat” landscape to “steep” landscape,

- Sqrt reward $R_{abs_sqrt}(v) = \sqrt{|v - v^*|}$
- Linear reward $R_{linear}(v) = \frac{v}{v^*}$
- Square reward $R_{abs_sq}(v) = |v - v^*|^2$
- Exponential reward $R_{abs_exp}(v) = \exp(-|v - v^*|)$

G. Automatic temperature tuning

Abdolmaleki et al. (2018) shows that we can tune the temperature variable λ in Equation (4) by primal-dual optimization, where the dual loss to update λ is

$$\lambda\epsilon + \lambda \log \text{sumexp}\left(\frac{Q(s, a^i)}{\lambda}\right) - \lambda \log N \quad (30)$$

First we compute the gradient of the second term, Let $f(\lambda) = \lambda \cdot \log \text{sumexp}(Q/\lambda)$.

Lemma G.1. *The gradient of $f(\lambda)$ with respect to λ is the Shannon entropy of the softmax distribution derived from Q , i.e.,*

$$\frac{\partial f(\lambda)}{\partial \lambda} = \sum_i p_i - \log p_i$$

where $p_i = \text{softmax}(q_i)$, $q_i = Q(s, a^i)$.

Proof. **1. Define the Function**

Let the vector $Q = [q_1, q_2, \dots, q_N]$. The function is:

$$f(\lambda) = \lambda \log \left(\sum_{i=1}^N \exp \left(\frac{q_i}{\lambda} \right) \right)$$

2. Differentiate with Respect to λ

We use the product rule $\frac{d}{dx}[u \cdot v] = u'v + uv'$. Let $Z = \sum_{i=1}^N \exp(q_i/\lambda)$. Then $f(\lambda) = \lambda \log(Z)$.

$$\begin{aligned} \frac{\partial f}{\partial \lambda} &= \frac{d}{d\lambda}[\lambda] \cdot \log(Z) + \lambda \cdot \frac{d}{d\lambda}[\log(Z)] \\ \frac{\partial f}{\partial \lambda} &= 1 \cdot \log(Z) + \lambda \cdot \frac{1}{Z} \cdot \frac{\partial Z}{\partial \lambda} \end{aligned}$$

Next, we calculate $\frac{\partial Z}{\partial \lambda}$:

$$\frac{\partial Z}{\partial \lambda} = \sum_{i=1}^N \frac{\partial}{\partial \lambda} \exp(q_i \lambda^{-1})$$

Using the chain rule:

$$\frac{\partial Z}{\partial \lambda} = \sum_{i=1}^N \exp \left(\frac{q_i}{\lambda} \right) \cdot \left(-\frac{q_i}{\lambda^2} \right)$$

3. Substitute and Simplify

Substitute $\frac{\partial Z}{\partial \lambda}$ back into the main equation:

$$\begin{aligned} \frac{\partial f}{\partial \lambda} &= \log(Z) + \frac{\lambda}{Z} \sum_{i=1}^N \exp \left(\frac{q_i}{\lambda} \right) \left(-\frac{q_i}{\lambda^2} \right) \\ \frac{\partial f}{\partial \lambda} &= \log(Z) - \frac{1}{\lambda} \sum_{i=1}^N \frac{\exp(q_i/\lambda)}{Z} q_i \end{aligned}$$

4. Interpretation as Entropy

We can express this result using the softmax probabilities p_i , where:

$$p_i = \frac{\exp(q_i/\lambda)}{Z} = \frac{\exp(q_i/\lambda)}{\sum_j \exp(q_j/\lambda)}$$

Substituting p_i into the gradient:

$$\frac{\partial f}{\partial \lambda} = \log(Z) - \frac{1}{\lambda} \sum_{i=1}^N p_i q_i$$

To see why this is entropy, recall that $H(p) = -\sum p_i \log(p_i)$. Since $\log(p_i) = \frac{q_i}{\lambda} - \log(Z)$, we have:

$$H(p) = - \sum_{i=1}^N p_i \left(\frac{q_i}{\lambda} - \log(Z) \right)$$

$$H(p) = - \frac{1}{\lambda} \sum_{i=1}^N p_i q_i + \log(Z) \sum_{i=1}^N p_i$$

Since $\sum p_i = 1$:

$$H(p) = \log(Z) - \frac{1}{\lambda} \sum_{i=1}^N p_i q_i$$

Conclusion:

The gradient is exactly the Shannon entropy of the probability distribution p :

$$\frac{\partial f}{\partial \lambda} = H(p) = - \sum_{i=1}^N p_i \log(p_i)$$

□

Interpretation of the whole gradient Therefore, we can interpret the gradient of (30) as

$$\epsilon + H(p) - \log N$$

where

- $\log N$ is the entropy of a uniform distribution, which is the **maximum possible entropy** of a discrete distribution on N variables. For our case, as we select $N = 32$, we have $\log N \approx 3.47$;
- $H(p)$ is the entropy of current reweighting distribution, $\text{softmax}(q_i/\lambda)$
- ϵ controls the gap between the current entropy and a fully uniform distribution.